METAL ATOM OXIDATION LASER

Richard C. Feierabend

NAVAL POSTGRADUATE SCHOOL
Monterey, California

THESIS

METAL ATOM OXIDATION LASER

by

Richard C. Feierabend

September 1976

Thesis Advisor: Daniel J. Collins

Approved for public release; distribution unlimited.

SECURITY CLASSIFICATION OF THIS PAGE (When Data Entered)

REPORT DOCUMENTATION PAGE

READ INSTRUCTIONS BEFORE COMPLETING FORM

1. REPORT NUMBER	2. GOVT ACCESSION NO. / 3. RECIPIENT'S CATALOG NUMBER
4. TITLE (and Subtitle): METAL ATOM OXIDATION LASER	5. TYPE OF REPORT & PERIOD COVERED: Master's Thesis; September 1976
	6. PERFORMING ORG. REPORT NUMBER
7. AUTHOR(s): Lieutenant Richard C. Feierabend	8. CONTRACT OR GRANT NUMBER(s)
9. PERFORMING ORGANIZATION NAME AND ADDRESS: Naval Postgraduate School, Monterey, California 93940	10. PROGRAM ELEMENT, PROJECT, TASK AREA & WORK UNIT NUMBERS
11. CONTROLLING OFFICE NAME AND ADDRESS: Naval Postgraduate School, Monterey, California 93940	12. REPORT DATE: September 1976
	13. NUMBER OF PAGES: 104
14. MONITORING AGENCY NAME & ADDRESS(if different from Controlling Office): Naval Postgraduate School, Monterey, California 93940	15. SECURITY CLASS. (of this report): Unclassified
	15a. DECLASSIFICATION/DOWNGRADING SCHEDULE

16. DISTRIBUTION STATEMENT (of this Report)

Approved for public release; distribution unlimited.

17. DISTRIBUTION STATEMENT (of the abstract entered in Block 20, if different from Report)

18. SUPPLEMENTARY NOTES

19. KEY WORDS (Continue on reverse side if necessary and identify by block number)

Metal Atom Oxidation Laser, Rare Earth Elements

20. ABSTRACT (Continue on reverse side if necessary and identify by block number)

This work represents a continuation of research investigating the feasibility of a metal atom oxidation laser. The work was done on the Naval Postgraduate School's metal-atom oxidation laser set-up which was designed and constructed as part of previous thesis research. The series of experiments was conducted with ten rare earth elements in a pure oxygen environment.

A brief discussion of the toxicity and handling character-

istics of the rare earth elements, the metal oxide laser system, and the possible metal deposition techniques is presented. The technique finally used in the metal deposition process and the difficulties incurred with this technique are also discussed.

Although no positive lasing action was noted, results from these experiments suggest further investigation is warranted.

Metal Atom Oxidation Laser

by

Richard C. Feierabend
Lieutenant, United States Navy
B.S.M.E., Cleveland State University, 1969

Submitted in partial fulfillment of the
requirements for the degree of

MASTER OF SCIENCE IN AERONAUTICAL ENGINEERING

from the

NAVAL POSTGRADUATE SCHOOL
September 1976

ABSTRACT

This work represents a continuation of research investigating the feasibility of a metal atom oxidation laser. The work was done on the Naval Postgraduate School's metal-atom oxidation laser set-up which was designed and constructed as part of previous thesis research. The series of experiments was conducted with ten rare earth elements in a pure oxygen environment.

A brief discussion of the toxicity and handling characteristics of the rare earth elements, the metal oxide laser system, and the possible metal deposition techniques is presented. The technique finally used in the metal deposition process and the difficulties incurred with this technique are also discussed.

Although no positive lasing action was noted, results from these experiments suggest further investigation is warranted.

TABLE OF CONTENTS

I. INTRODUCTION

The metal atom oxidation laser makes use of an exothermic, atom diatom exchange, chemical reaction as the means of achieving the population inversion necessary for lasing action. The energy resulting from the exothermic chemical reaction, goes into pumping the products of the reaction to highly excited levels. Briefly, the basis for these experiments is the chemical reaction $M+XY \rightarrow MX^*+Y$, first suggested by Polanyi. He theorized chemical laser action was possible from the reaction provided M was an alkali metal atom (potassium, sodium, etc.) and XY was a covalent halogen or halide (fluorine, chorine, etc.); XY* was the resulting metal halide from which lasing action was expected. This theory has recently been extended to include most reactive metals for M and almost any gaseous oxidizer for XY. As an example, the reaction $Al+F_2$ AlF*+F has produced lasing action.

Metal atom lasers are not new. The first metal vapor laser was invented at Columbia University in 1961. This metal vapor laser was based on cesium vapor. The original metal vapor lasers were of the pulsed type, but later advancements led to the continuous wave (CW) laser. In the first metal vapor CW laser, helium and cadmium were used and an electric

current was used to pump the laser. (Ref. 1)[1]

In recent years, Rice, Beattie et al at the Los Alamos Scientific Laboratory reported they were able to obtain IR lasing action using the metal atom oxidation principle from CO, TiO, VO ZrO, LiF, MgF and other diatomic molecules (Ref. 2). "The important possible applications of this class of lasers are development of low gain systems operating on triplet-singlet transactions and capable of very large energy storage for pulse laser applications, and development of high efficiency CW lasers in the infrared."[2]

The ten rare earth elements that were considered for this investigation were lanthanum (La), praseodymium (Pr), neodymium (Nd), samarium (Sm), gadolinium (Gd), terbium (Tb), dysprosium (Dy), holmium (Ho), erbium (Er), and ytterbium (Yb). Basic properties of these elements are given in Table 1. Only terbium was actually used in this work.

The rare earth elements have been considered because of

---

[1] Laser action is possible in elements which have a high vapor pressure, e.g. gases at room temperature. It is also possible to obtain reasonably high pressure even for metals which do not have vapor pressures high enough at room temperature. This is accomplished by heating the metal in a vacuum whereby the vapor pressure is increased, and then the pressure of the metal vapor may be high enough to obtain laser action by electron impact excitation; thus the name metal vapor laser.

[2] Rice, W. W., Beattie, W. H., Metal Atom Oxidation Laser, p. 1

their low-lying electronic states and stability of their compounds; this is an essential requirement of the chemical product MX* in the reaction M + XY→MX* + Y.

II. TOXICITY AND HANDLING OF THE RARE EARTH ELEMENTS

All the materials used in the experiments are at least 99.9% pure. They were purchased from the Ventron Corporation of San Leandro, California.

The first task before beginning any experiments was to determine the toxicity of each of the ten elements and their compounds and what precautions had to be taken when handling them. While the rare earths have been used extensively in industry, particularly in the electronic and metallurgic disciplines, the information concerning the toxicity and other information of these elements is relatively scant. The little information found in Sax's Dangerous Properties of Industrial Materials (Ref. 3) appears to confirm this. A library search and references supplied by the Rare Earth Information Center at the Iowa State University provided additional sources of information. While most of the observations in these sources are made from a pharmacological point in view, they nevertheless give an insight as to the relative toxicity of some of the rare earths and their compounds.

Vincke and Oelkins administered rare earth chlorides to mice subcutaneously. Their studies showed the LD_{50}[3] of

---

[3] Lethal dose 50, or medium lethal dose, is written LD_{50} and is used when the response that is being investigated is the death of the experimental animal. Therefore, LD_{50} is the dose which is fatal to 50% of the test animals.

these substances varied between a low of 2.5 gm/Kg for praseodymium chloride to a high of 4 gm/Kg for lanthanium and neodymium chloride; administered in this manner, the toxicity was low. Upon intravenous injection of the same compounds, the LD_{50} level was considerably smaller, of the order of 200 - 250 mg/kg. Studies were also made with mixtures of dusts of rare earth fluorides and oxides administered intratracheally and by inhalation. Some of the test animals (guinea pigs) died of pneumonia; the others were killed for autopsy 8 to 156 weeks later. No fibrotic effect was noted in any of the cases. Other experiments using dusts of yttrium, neodymium and cerium oxides were also made. These dusts were administered intratracheally to white rats. The investigation showed that these oxides "exert a distinct pathological effect of the respiratory tract."[4] Each of the oxides that was studied had an effect that was quantitatively and, in some cases, qualitatively specific. Yttrium oxide had the most marked fibrotic effect. The effect of neodymium oxide was similar to that of yttrium oxide but milder. Cerium oxide was the least damaging of the three. With regard to the"aerosols of the oxides of yttrium, neodymium and other rare earth elements, it is essential that measures

---

[4] Mogilevskaya, O. Ya, Raikhlin, N. T., Toxicalogy of the Rare Metals, p. 140

be taken to remove the aerosols formed."[5] Thus, to prevent inhalation of any dust particles, an industrial face mask was worn while handling the elements. As an added precaution, the exhaust from the vacuum pump was vented to the atmosphere via an exhaust hood.

Further research indicated the rare earth elements react primarily with moisture; for this reason plastic gloves were worn whenever handling the elements.

Another precaution which was not mentioned above but nevertheless is very important is the fact that several of the elements may be pyrophoric under certain conditions (several of the preliminary metal films "sparked" when the vacuum system was opened to the atmosphere (Table 2)). If this should occur, the system should be cycled so that the seal at the base of the bell jar is not broken; this should allow the vacuum pumps to purge the bell jar and prevent any fumes from entering the work area.

Based on the information that was found, working with the rare earths presents little hazard to the individual provided the precautions mentioned above are followed.

---

[5] Mogilevskays, O. Ya, Raikhlin, N. T., Toxicalogy of the Rare Metals, p. 140

III. SYSTEM DESCRIPTION

The metal atom oxidation laser system was built as part of previous thesis work (Ref. 4) and is similar in appearance and design to the system currently being used at the Los Alamos Scientific Laboratory. A brief description of the elemental parts of the system follows. A somewhat more detailed discussion can be found in Ref. 4.

A. OPTICS

The optical cavity consists of two, one-inch diameter gold surfaced mirrors, each with a 10-meter radius of curvature. Each mirror is placed in a three degree of freedom mount; the distance between the mirrors is approximately 140 cm. A one-mm hole in one of the mirrors provides output coupling to the detector (Fig. 1).

B. EXPERIMENTAL TEST SECTION

The experimental test section is comprised of: (1) two high-voltage (HV) heads, (2) a 24 cm x 2.2 cm I.D. Pyrex tube (laser tube) which separates the HV heads, and (3) the necessary vacuum/gas and electrical connections (Fig. 2).

Each high-voltage head is made of monel and type 321 stainless steel and is assembled in three separate sections (Fig. 3). The outward facing end sections contain the NaCl windows which are mounted at the Brewster angle. The center section is cylindical in shape and provides a

place for the electrical and vacuum/gas connections in addition to containing the explosion baffles. The inward facing end plates provide a means of mounting the Pyrex laser tube. The entire assembly (high voltage heads and Pyrex tube) is mounted on blocks of insulating material, and is held in place with set screws that screw into the HV heads; this allows each HV head to slide independent of the other thus providing a rapid means of interchanging Pyrex tubes.

C. ASSEMBLAGE

The optical cavity and the experimental test section are mounted on a two-meter optical bench. Besides these elements, a Santa Barbara Research Corporation (SBRC) Ge-Au detector, capable of measuring in the 1.0 to 11.0 micron range, is placed at the "coupling-mirror" end of the bench. A plexiglass enclosure surrounds the entire system (the enclosure allows the experiments to be conducted in a nitrogen atmosphere). Also enclosed is the system's gas/vacuum solenoid valves and associated tubing (Fig. 4).

D. GAS/VACUUM SYSTEM

The vacuum and gas handling system was designed to provide:

1. A remote means of evacuating the laser tube and subsequently filling it to a specific pressure with a known gas such as oxygen, chlorine, or fluorine.

2. A means to purge and exhaust to the atmosphere, any residual gaseous products at the completion of each experiment.

3. A means to provide for a nitrogen atmosphere in the plexiglass enclosure.

Ten Skinner solenoid valves (Fig. 5) give the capability to remotely evacuate the laser tube and then to fill it with a known gas at a specific pressure. 1/4-inch stainless steel tubing is used throughout the vacuum system with the exception of the section between the vacuum isolation valve and the Welsh mechanical roughing pump; in this section 1/2-inch stainless steel tubing is used. These valves are operated electrically from a portable control panel. A system schematic is indicated on the front face of this panel. Lights on the panel represent relative positions of the valves in the system. Toggle switches adjacent to each light opens or closes the respective valve: light on-valve open; light out-valve closed (Fig. 6).

System pressure is monitored with an MKS Instruments, Inc., Baratron - 170 pressure meter with digital readout (Fig. 7).

E. ELECTRICAL SYSTEM

The high voltage electrical system includes several oil filled capacitors, a New Jersey Electronics Model HA-51 variable power supply, system control boxes and circuitry, and a pulse triggering arrangement.

The capacitor bank consists of several 1.5 to 7

microfarad oil-filled, 25 KV capacitors. These can be connected either in series or parallel to give a wide range of effective capacitances. Only one 7 microfarad capacitor was used for the series of experiments. A plywood enclosure is built around the capacitor bank.

A New Jersey Electronics Model HA-51 variable power supply (Fig. 8) charges the capacitor bank to the desired voltage. Charging rate and level can be selected with the Variac on the power supply panel; progress of the charging sequence is easily monitored with the meter on the front plywood panel (Fig. 9).

Control for charging the capacitor bank is accomplished with a small, portable control box (Fig. 10). A series of switches on the box controls the charging and dumping processes. Four lights along the top indicate the status of the system:

1. System Pwr on/off
2. Charging
3. Ready
4. Dump

The box is connected to the Charging Control Circuitry with a 10 ft. cable.

The charging control circuitry is located on a panel inside the capacitor bank enclosure. The main power switch for the charging control circuit is mounted on the outside of the enclosure next to the high voltage selection meter

(Fig. 9). The H.V. selection meter is a 0-20mA ammeter connected to function as a 0-20KV voltmeter and incorporates a limit adjustment which: 1) stops capacitor charging when the desired voltage is reached and 2) lights the "ready" light through a system of relays. Below the main power switch is the primary dump switch. (In order to charge the system, a copper drop plug must be lifted away from the grounding strap. This is accomplished by pulling the string on the top of the plywood enclosure to reset the solenoid core. Momentarily hitting the primary dump switch disrupts power to the solenoid holding the core in place; this in turn allows the copper drop plug to fall across the capacitor grounding strap thereby grounding the system. Should the dump switch on the portable control panel be selected first, it is likely that the Kilovac vacuum switch will be destroyed.)

The high side of the capacitor bank is connected directly to one of the HV laser heads. The low (ground) side of the bank is connected to the other HV head through a spark gap which functions as a high voltage switch. Connections are made with 3/8-inch copper tubing wrapped with electrical tape.

The spark gap (Fig. 11) consists of two electrodes that can be separated from zero to two inches (note that if the gap is too close and a high enough voltage is selected, premature ionization of the gas will occur). Each electrode

is made up of a 1-1/4-inch copper hemisphere on a 5/8-inch copper stem. The copper tubing from the HV head is connected with a set screw to one electrode stem, the other electrode stem connects to the copper tubing leading to ground. A tungsten electrode placed in the gap between the hemispheres acts as a firing trigger (Fig. 12). The tungsten electrode is in series with a 100-Kohm high voltage resistor. A plexiglass shell surrounds the copper and tungsten electrodes.

An ILC PG-10 pulse generator (Fig. 13) provides a voltage triggering pulse to the spark gap and a voltage "sync" signal to the instrumentation system. The trigger pulse is directed first through an ILC Model T-105 pulse forming network before reaching the spark gap. This pulse forming network consists of an 8- microfarad, 500V oil filled capacitor and a 60:1 step-up pulse transformer.

F. INSTRUMENTATION

The instrumentation set-up for the experiments includes detectors, biasing circuits, amplifiers, oscilloscopes, a current measuring transformer and a high voltage probe.

A Santa Barbara Research Corp. (SBRD) Ge:Au detector (Fig. 14) was used to measure the IR radiation. Visible radiation was monitored with a photomultiplier. The output of the IR detector was fed into a Tektronix Type 549 storage oscilloscope with a Type 1A6 differential amplifier plug-in unit. The output of the photomultiplier is fed

into a Tektronic Type 53/54D high gain differential amplifier plug-in unit which feeds into a Tektronix Type 545 oscilloscope (Fig. 15). Copper shielding around the output leads of each detector and a capacitance network are needed to reduce the interference from the spark gap.

Capacitor voltage during each experiment can be monitored with a Tektronix P6015 high voltage probe connected to the high side of the capacitor. The signal is fed into the 53/54D high gain differential amplifier.

The circuit current is measured with a 5000:1 current transformer. Neither the high voltage probe nor the current transformer was used during these experiments.

Both oscilloscopes were triggered with the PG-10 "sync" pulse. A variable delay in the spark gap trigger circuit allows the scopes to be triggered 10 microseconds prior to the spark gap being triggered.

Tektronix series 125-1.9-1:0.85 magnification Polaroid cameras using polaroid type 107, 3000 speed film provided a permanent record of each experiment.

IV. METAL DEPOSITION - BACKGROUND

Reference 2 states: "If a quantum efficiency of one 10 μm ir photon per metal atom and a reaction rate of 10^{13} cm/Mole-sec are assumed, the metal atoms would have to be present in a concentration of 5.5×10^{12} cm^{-3} to produce the needed power from a 10 cm^3 volume."[6] The "needed power" is the minimum power from the laser device to overcome optical losses and "to be capable of running under non-ideal conditions often needed for obtaining kinetic information";[7] (this power should be at least 10 microwatts). "Electrical explosion of metal wires and foils have been known to produce many orders of magnitude higher density than the required 10^{12} cm^{-3}".[8]

As previously mentioned, ten rare earth elements were to be studied. The ten elements came in a variety of shapes and sizes ranging from short solid rods (approximately 2.5cm x 1.0cm O.D.) to this metal chips. The problem that was to be resolved then, is to somehow transform the rare earth elements in their acquired state into a form that could be worked with easily, e.g., a thin film.

---

[6] Rice, W. W., Beattie, W. H., Metal Atom Oxidation Laser, p. 1

[7] Ibid #6

[8] Ibid #6

The simplest solution would have been to get wires or thin foils of each of the elements. But because of either the cost or the non-availability of the elements in one of these forms, this solution was discarded.

An effective method introduced in 1969 by Karev et al. (Ref. 5) was to reduce the oxides of several rare earths with La or Zr in the form of chips or shavings, "the metal thereupon being evaporated and condensed on a cold substrate in another part of the apparatus".[9] This method, too, was discarded because of the lack of the necessary equipment.

It was finally decided to try to deposit the metals as a thin film by evaporation. The decision was based primarily on the equipment resources available at the Naval Postgraduate School and on the requirement that the film was to be deposited on the inside of a 22 mm I.D. Pyrex laser tube.

Evaporation is a relatively simple technique for depositing materials. The material to be applied is heated to a temperature where its vapor pressure is at least 10^{-2} torr. The molecular rays of the material leave it and travel relatively unobstructed until they reach the substrate

---

[9] Karev, V. N., et al, from abstract of report; Air Force Systems Command FTD-MT-24-93-71, Foreign Technology Division, Wright-Patterson AFB, Ohio, Thin Films of the Rare Earth Metals

surface. The degree of vacuum required is such that the mean free path of the residual gas molecules is greater than the distance from the source to the substrate. The vapor pressure-temperature relationship and the potential reactions with the heating material must also be considered. Table 3 shows evaporation temperatures for a few of the rare earths and the resulting evaporation rates. The temperatures are those for vapor pressure of .01 torr; Dushman's equation was used for these calculations.[10]

For film formation, the deposition rate and substrate temperature are also essential parameters. Substrate temperature "determines the surface mobility of the arriving film atoms, in conjunction with the forces between film and substrate atoms. The surface mobility also influences the number of collisions among film atoms on the surface of the substrate. Since nuclei for the formation of crystallites can result from such collisions - at least in the initial stages of film formation - both substrate temperature and the rate of deposition, i.e., the number of atoms arriving, are important in determining the film structure. The material of film and substrate will again enter the considerations since the binding forces between the atoms of the film and those of the substrate determine the mode of growth of the film

---

[10] Powell, Oxley, Blocher, Vapor Deposition, p. 224-225

(continuous, island formation, etc.)."[11] It was recommended that the substrate be heated to an elevated temperature above room temperature to enhance the film formation of the elements. This was accomplished automatically with the heat from the tungsten filament; the exact substrate temperature was now known, however.

Surface preparation and roughness of the substrate is another area of concern. The cleaning of the substrates to be coated by physical vapor deposition is usually more difficult than that required for other deposition processes such as electrodeposition or chemical vapor deposition. As was mentioned previously, the laser tube was made from a Pyrex tube. Since Pyrex is a very smooth material, it was assumed that most of the surface contamination could be removed with acetone. This method of cleaning worked well in all cases, provided a new Pyrex tube was used each time material was to be deposited and no attempt was made to reuse the same tube.

Baking the Pyrex substrate to remove contamination was also considered. However, it was not done because of the possibility of depositing a residue of carbonaceous material on the substrate (from the cracking of the hydrocarbon pump oil vapors).

Thus, the only substrate surface preparation done was to wipe the inside of the tube with an acetone saturated swab.

---

[11] Behrndt, K. H., Thin Films, Chapter 1, p. 9

V. DEPOSITION SET-UP AND PROCEDURE

Past studies have indicated that the rare earth elements are active getters, particularly for oxygen and hydrogen. It was, therefore, necessary to perform the deposition of each element in as high a vacuum as possible. A VEECO VE 401 Evaporation unit (Fig. 16), capable of maintaining a pressure of 10^{-6} - 10^{-7} torr, was used in the deposition of the elements. In private conversation, the personnel at the Rare Earth Information Center of the Iowa State University recommended depositing the metals in a vacuum of 10^{-8} - 10^{-9} torr; this would insure that the elements being deposited would be of relatively high purity. An attempt was made to further improve the vacuum in the chamber by placing a 0.25 mm zirconium wire between a second set of electrodes. After reaching the minimum pressure of the system, the zirconium wire was heated by passing an electric current through it. It was hoped that the hot zirconium wire, acting as a gettering material, would further reduce the oxygen partial pressure. After the pressure had stabilized, the current was turned off and the deposition process continued. (It should be noted that the pressure gauge on the VE 401 unit did not provide accurate pressure measurement below the 10^{-6} torr range.)

Figure 17 and 18 show the Pyrex tube/filament setup for the actual metal deposition procedure; included is the

filament, a slotted Pyrex shield, and the laser tube.

Three-strand, 0.025-inch tungsten, loose-lay wire from the R. D. Mathis Company, Long Beach, California was used both to support the rare earth element nodals and also to act as the heat source. Tungsten, tantalum, and molybdenum are three commonly used heat sources. Of the three, tungsten has the highest melting point (6170°F) compared with tantalum (5425°F) and molybdenum (4730°F). D. H. Dennison et. al. conducted a series of experiments with the liquid rare-earth elements to determine the solubility of tantalum and tungsten in each. Their data showed tungsten was a better refractory material "since tungsten is less soluble than tantalum in the liquid rare-earth metals by a factor from 2 for Sc and the heavy lanthanides to 10 or greater for the light lanthanides".[12] (Ref. 6)

Table 2 lists the rare earth elements used in the preliminary experiments. Also included in the table is copper, which was used to verify that the proposed deposition technique was plausible; the results will be discussed shortly. The current in the table is the current used for the deposition process. In most cases, it was also the current at which evaporation was first observed. The VE 401

---

[12] D. H. Dennison, et.al., Journal of the Less Common Metals Vol II, "The Solubility of Tantalum and Tungsten in Liquid Rare-Earth Metals", p. 423

unit bus bar arrangement shown in Fig. 19 was used in all the depositions. A wire diameter-current-temperature nomograph is shown as Fig. 20 and was used to give an approximate wire temperature during the deposition process.

The particular rare earth element to be deposited was either sawed into small pieces with a clean jewelers hacksaw or cut with a pair of "nibblers". The physical size and shape of each piece varied depending on the adeptness of the individual doing the sawing/cutting. Average length of each piece was 3 - 4 mm; the size was purposely kept small so that they could be placed between the strands of the tungsten filament. Care was taken not to contaminate the metal with any grease or other foreign material on the tools.

Approximately 3.5 cm of length on either end of the 30 cm long tungsten filament was used to clamp the filament to the heater posts of the VE 401 evaporation unit. The remaining length provided the support for the pieces of the rare earth element. The pieces were placed between the filament strands on 1 cm centers. Major disadvantage of this method is that a uniformly thick film is not produced. Rather, there were alternating thick and thin portions along the entire length of the surface because of the over-lapping effect from the metal pieces on either side of any one particular node. By placing the pieces close enough together, it was hoped that a more uniformly thick film would

be obtained. After placing all the rare earth element pieces on the filament, the components in the deposition process were placed in the vacuum system and assembled as shown in Fig. 21. The system was then pumped down to its minimum pressure. Further system pressure reduction was made with the heated zirconium wire (i.e., oxygen partial pressure).

Heating, as evidenced by the orange-red glow of the tungsten filament, first started at the center of the filament and progressively spread in both directions as more current was applied (current was controlled with a rheostat and monitored with an ammeter built into the system). A direct result of this uneven heating was the fact that more material was deposited in the center of the laser tube than on the ends.

Before deposition with the rare earths began, a preliminary experiment was made with copper as the test material to determine whether or not this unevenness would be critical to the success of our experiments. The thickness comparison was made by noting the optical density along the length of film; in the center no light was able to pass through the film while at the ends it was possible to see through it. The laser tube was then placed in the system and electrical connections made to the HV laser heads. The connections were made with silver conducting paint and short lengths of resistor

leads. After checking the continuity with an ohmeter, a high voltage (10KV) charge was applied. The result was that the copper film completely vaporized. This simple experiment served two purposes. The first was that this led to the belief that the extra build-up of material was not critical to the experiments; and secondly, the experiment demonstrated that we could vaporize a film with our system.

As the filament became hotter, it had a tendency to sag or twist and then, in most instances, to come in contact with the Pyrex tube. The direct result of this was heat being conducted away from the filament at that point, which resulted in poor film production in the same area. By placing ceramic beads along the filament the heat loss was reduced but not totally eliminated as had been hoped.

Once evaporation of the metal was observed, the current was not normally increased (a few times, however, it was necessary to increase it in order to melt the metal near where the filament was touching the sides). Depending on the circumstances, the time to complete the deposition process from time evaporation was first observed, was between thirty seconds and one and one half minutes.

After completion of the process, the tube was allowed to cool several minutes. When the system was opened to atmosphere, care was taken to note any unusual occurrences (e.g. flashing, oxidation, etc.) and to be prepared to take any precautionary steps.

VI. EXPERIMENTAL RESULTS

The first series of experiments were to have been made with holmium, dysprosymium, erbium, terbium, and gadolinium; these elements were chosen primarily because of their slow oxidation rates.

The first element of the group to be tested was terbium. In our preliminary deposition experiments it was the easiest element of the five to work with and the only element to completely wet the filament.

Terbium came in the form of thin, brittle chips. It was cut into small triangular pieces approximately 3 - 4 mm in length and 2 mm wide with a pair of "nibblers". The pieces were then placed between the strands of the tungsten filament. The filament along with the remainder of the equipment (laser tube, etc.) was assembled and placed in the VE 401 evaporation unit.

The experiments discussed in the remainder of the section were done with terbium; because of the time element, no experiments were conducted with the other four elements.

A. EXPERIMENT I

Deposition progressed smoothly until the filament began sagging; it continued to sag until it came to rest on the side of the slotted Pyrex shield. Metal was deposited on both ends of the laser tube but not in the center due to heat conduction away from the filament at the point of con-

tact. Silver conducting paint was used to complete the strip.

The tube was placed in the laser system and electrical connections to the high voltage heads were made using silver conducting paint and short lengths of conducting wire. Continuity was checked with an ohmeter.

When the manual trigger switch on the PG-10 control box was depressed, only the silver conducting paint was vaporized and not the terbium. The voltage was 10 KV (350 joules) and the pressure approximately 29 torr. Figure 22 is the trace of the IR detector output. Note the blank portion between forty microseconds and one hundred ten micro-seconds. Further investigation of this segment is necessary to determine whether lasing action was responsible for the observed output. The photomultiplier output was not photographed because a second oscilloscope was not available. Figure 23 shows the laser tube after the experiment.

B. EXPERIMENT II

The second deposition attempt was slightly more successful. There still remained the problem of the tungsten filament sagging at high temperatures and coming in contact with the side of the tube. This time, however, more current was allowed through the filament to compensate for the heat loss. The terbium strip was completed but the tube cracked in the process.

Not wanting to waste the material, the tube was carefully placed in the system and the crack covered with a rubber-like sealant.

After the tube was placed in the system and electrical connections made, the resistance was measured. The resistance of the strip was measured between the high voltage laser heads; it measured approximately 1000 ohms and decreased as the silver conducting paint dried (the minimum resistance observed for the eight experiments was about 200 ohms). The voltage was set at 10 KV and the pressure at 22.75 torr.

Approximately seventy-five per-cent of the material vaporized when the manual trigger switch was depressed. The remaining amount did not appear to physically change (i.e. color, shape, etc.).

No record of the output was made since the trace of the oscilloscope to which the IR detector was connected drifted off the face of the scope. The photomultiplier oscilloscope failed to trigger.

C. EXPERIMENT III

Several ceramic beads were placed at equal intervals along the filament in order to keep it from coming in contact with the side of the tube. This worked very well; the material was deposited more uniformly than in the previous two attempts. The only unusual characteristic of this film was two "crystalline" sections directly opposite

each other. Resistance of the strip again remained at 1000 ohms and decreased as the silver paint dried.

The tube was connected as had been done before. The voltage for this experiment was selected as 15 KV (787.5 Joules) and the pressure stabilized at 20.22 torr.

As the voltage increased toward 15 KV, the system fired prematurely (the spark gap was set to close for such a high voltage). The pressure dropped to 19.84 torr. Approximately 95% of the film vaporized (Fig. 24).

The IR detector output (Fig. 25) did not appear to detect any lasing phenomenon, only an electrical ringing effect. Note the trace begins at about forty microseconds; what is happening, i.e., the presence of lasing, between zero and forty microseconds must still be determined. The photomultiplier trace (Fig. 26) appears blank, but between 180 microseconds and 200 microseconds there is a faint diagonal line crossing the x-axis at about 196 microseconds.

D. EXPERIMENT IV

The material was again deposited on the laser tube without any difficulty. The tube was placed in the system and the electrical connections were also made without any problems; the resistance still measured about 1000 ohms. The voltage was selected as 12 KV (to prevent premature firing) and the pressure at 14.78 torr. Only a small amount of material vaporized however when the trigger switch was depressed (Fig. 27).

The IR output (Fig. 28) shows what appears to be a damped wave form with equally spaced spikes. This was thought to be electrical in nature and not a direct result of the reaction. The "grass" in the first thirty microseconds of the photomultiplier output (Fig. 29) was assumed to be the result of the spark gap firing.

E. EXPERIMENT V

Both the slotted inner tube and the outer laser tube broke during the deposition process. This was a direct result of a combination of factors: The first is the concentration of heat at the point of contact of the ceramic bead on the side of the Pyrex tube and the second is the snug fit of the two tubes (i.e., there was not room for adequate thermal expansion of the slotted tube).

The second attempt was slightly more successful. The terbium strip was deposited on the laser tube but the second slotted tube cracked in the process. The resistance of the strip again measured something less than 1000 ohms.

Figure 30 is the IR detector output. The blank portions are thought to be the result of lasing action; however, further investigation is required to either affirm or disprove this postulation. The photomultiplier output is shown as Fig. 31; the quality of the photograph is poor and therefore of little apparent value.

The voltage for this experiment was 12 KV (504 Joules) and the pressure about 19.44 torr; there was little noticeable pressure change. Figure 32 shows the tube after the firing.

F. EXPERIMENT VI

Since there were no more slotted tubes to be used, it was decided to coat the entire inside of the laser tube with terbium. This was accomplished without difficulty. The resistance was the same as before.

No record of the test was made, however, because of a careless error and an oversight on the part of the experimentor. The IR output looked similar to that of experiment V. However, before a record of the trace could be made, the oscilloscope was turned off and the output lost. The photomultiplier was not used in this experiment because of an oversight error.

G. EXPERIMENT VII

Again the entire inside of the tube was coated with the metal. The resistance measured the same as before, the voltage was selected again at 12 KV and the pressure was set at 15 torr.

The IR output (Fig. 33) looks very similar to that of experiment IV. The spikes are thought to be system noise detected because of an improperly assembled instrumentation set-up; this could explain the similar output in experiment IV. The photomultiplier output (Fig. 34) illustrates an

unusual occurrance in the first 65 microseconds. Figure 35 shows the laser tube after the experiment.

H. EXPERIMENT VIII

The last experiment was again made with a completely coated tube. During the deposition process a crack developed in the laser tube because of filament contact with the side of the tube. Nevertheless, the tube was placed in the system and the necessary electrical connections made. The voltage was again selected at 12 KV, the pressure, however, steadily increased because of the crack (at the time of firing the pressure was approximately eight mm Hg).

Figure 36 is the output from the IR detector. Note the blank portion starting about fifty-five microseconds and the faint diagonal trace at about ninety-five microseconds. No photomultiplier output was obtained.

VII. CONCLUSIONS AND RECOMMENDATIONS

A series of eight experiments were conducted; the rare earth element in each experiment was terbium. This element was as excellent choice to begin our experiments with in that it was easily handled and cut into the proper size for the deposition process. The remaining nine rare earth elements may be considerably more difficult to work with due either to the form they are in (some elements are formed into short cylindrical pieces) or their hardness. For this reason, a slight modification in the deposition process is advisable if it is found that the present method proves too difficult.

One possible alternative might be to use a tungsten mesh in place of the three strand tungsten filament. In this manner, nearly all the pieces of the element would be utilized and not just the ones that fit snuggly between the filament strands (with the present method the smaller pieces normally are not used because they can not be made to stay on the filament).

It may be advantageous to apply a method similar to the one suggested by Karev (Ref. 5) to produce the thin film. If this would not involve a great deal in time or expense, serious consideration should be given to this method.

The present method of deposition does not allow for measurement of the film thickness during or after the deposi-

tion process. If it is desired to have the film on the inner surface of the laser tube, as is the case now, and if the quantity of metal is desired, a method of thickness measurement must be devised. One such method recently suggested is to use an electron microscope. The feasibility of this method has not been explored but the idea merits more attention. A second alternative might be to use separate long, narrow Pyrex slides (similar to microscope slides) if the necessity for the element to be on the inner surface is not so critical that it can be relaxed. This method has several advantages: 1) more than one slide can be made during the deposition process; 2) thickness of the film can be easily monitored, such as with a Sloan thickness monitoring device or some other similar device and 3) a more even film will be made since the distance between the filament (or a mesh) and the substrate can be varied to determine the optimal distance for both deposition uniformity and thickness monitoring. Thickness measurements using optical transmission or reflection characteristics of the film, by observation of interference patterns and colors, should also be considered.

The filament in all the cases began sagging or twisting as more current was directed through it. A seemingly satisfactory solution was to place three or four ceramic beads along the filament. It should be noted that in several

instances when the beads came in contact with the sides of the tube, a sufficient amount of heat was conducted away from the filament to cause degraded metal deposition in that area and in a few cases cracking of the tube(s). Until a better solution is found, the ceramic beads are still the best choice to prevent the filament from coming in contact with the Pyrex surface.

The alignment procedure discussed in Appendix C, while satisfactory, is not the best possible procedure. The procedure discussed in Ref. 2 is a much better method and consideration should be given to use the same or similar method.

After several experiments the inside of the NaCl windows became coated with the products of the chemical reactions, which made it increasingly difficult to align the system. Changing the windows after two or three experiments would make aligning the system much easier and may even enhance the output to the detector.

While only a cursory set of experiments with terbium have been made, there remairs a great many other conditions (i.e. voltage/pressure combinations) that need to be examined. This applies not only to terbium but also to the other rare earth elements. Consideration should also be given to using other gases besides oxygen, such as chlorine or fluorine, but only after the necessary safety precautions have been taken.

Although we were not able to achieve positive lasing action from our experiments, there remains sufficient optimism resulting from these experiments, and at the Los Alamos Scientific Laboratory, to warrant continued investigation into the possible lasing properties of the rare earth elements as applied to the chemical reaction $M + XY \rightarrow MX^* + Y$.

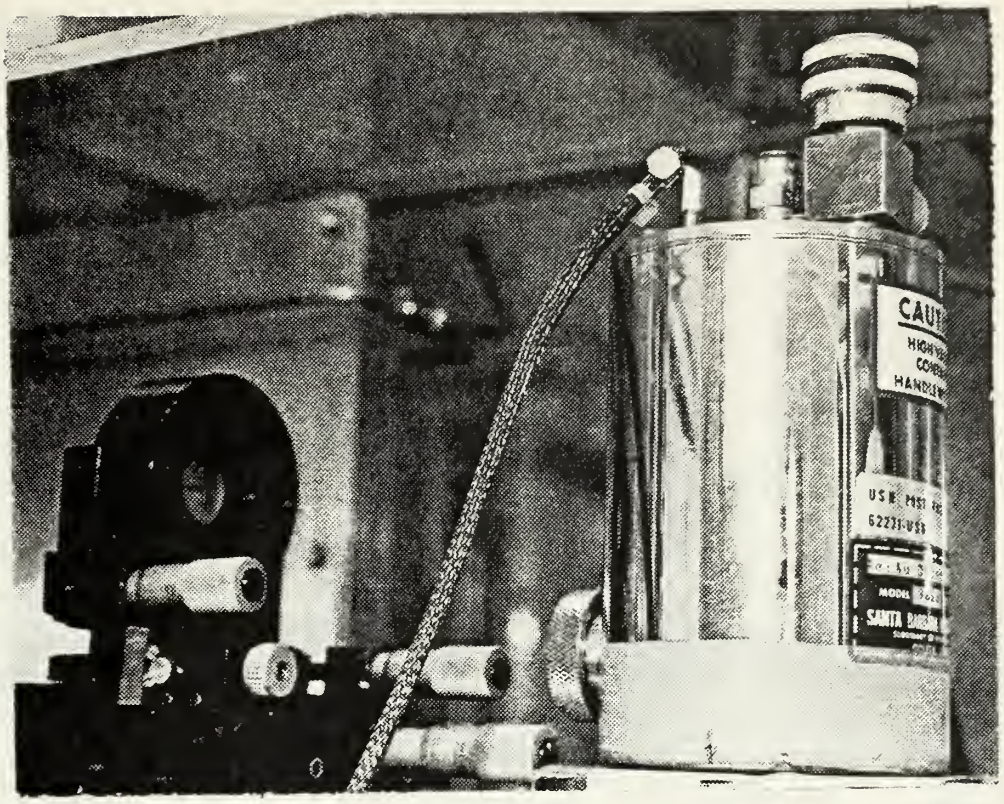

Fig. 1 Output coupling mirror mounted in three degree of freedom mount and IR detector

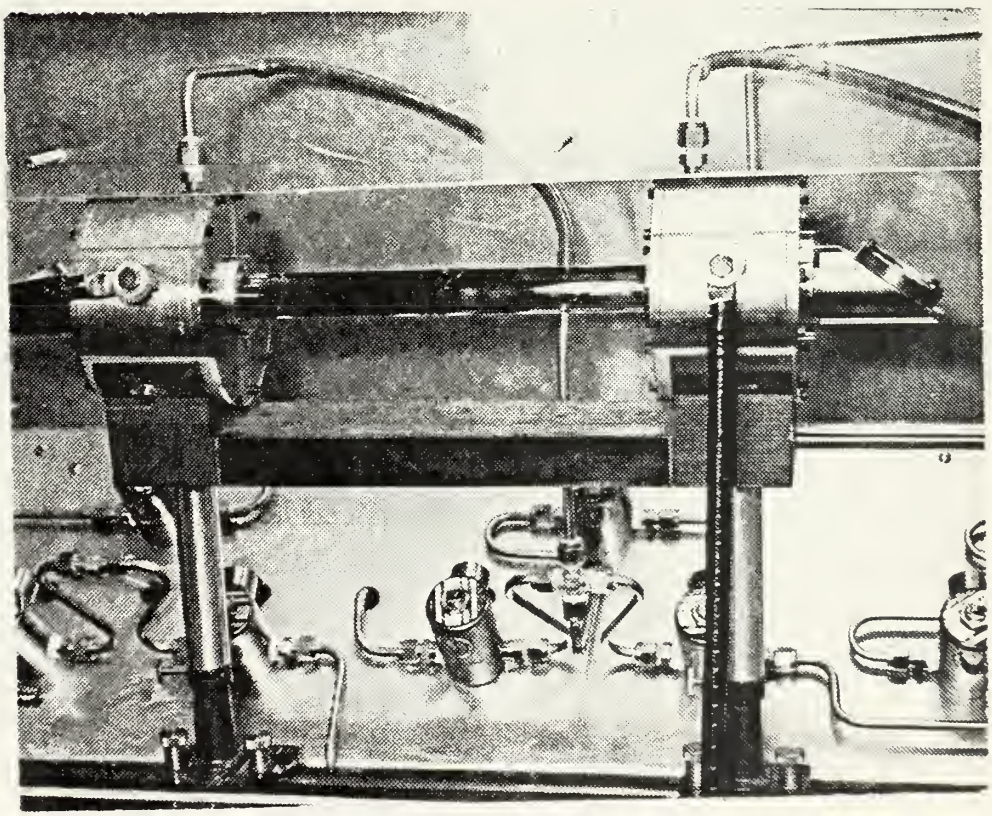

Fig. 2 Experimental Test Section

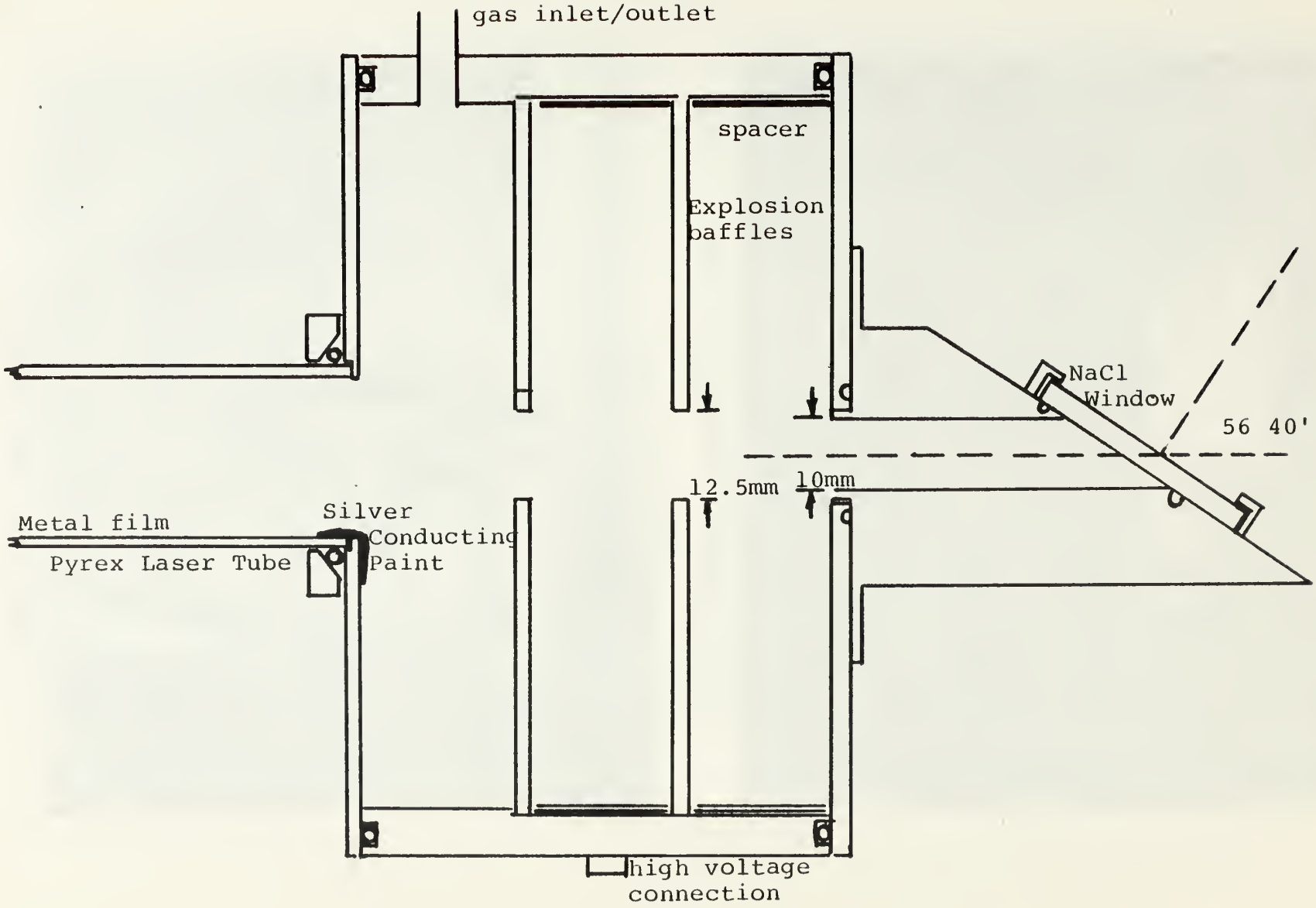

Fig. 3 High Voltage Head Detail

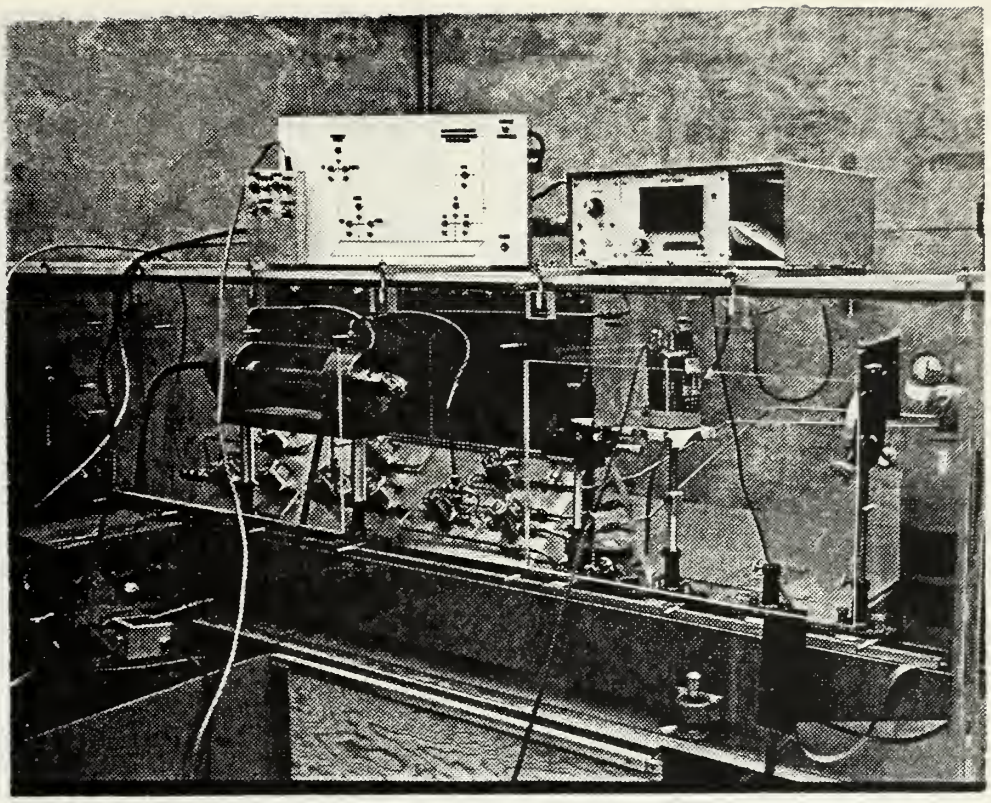

Fig. 4 Metal Atom Oxidation Laser Set-up

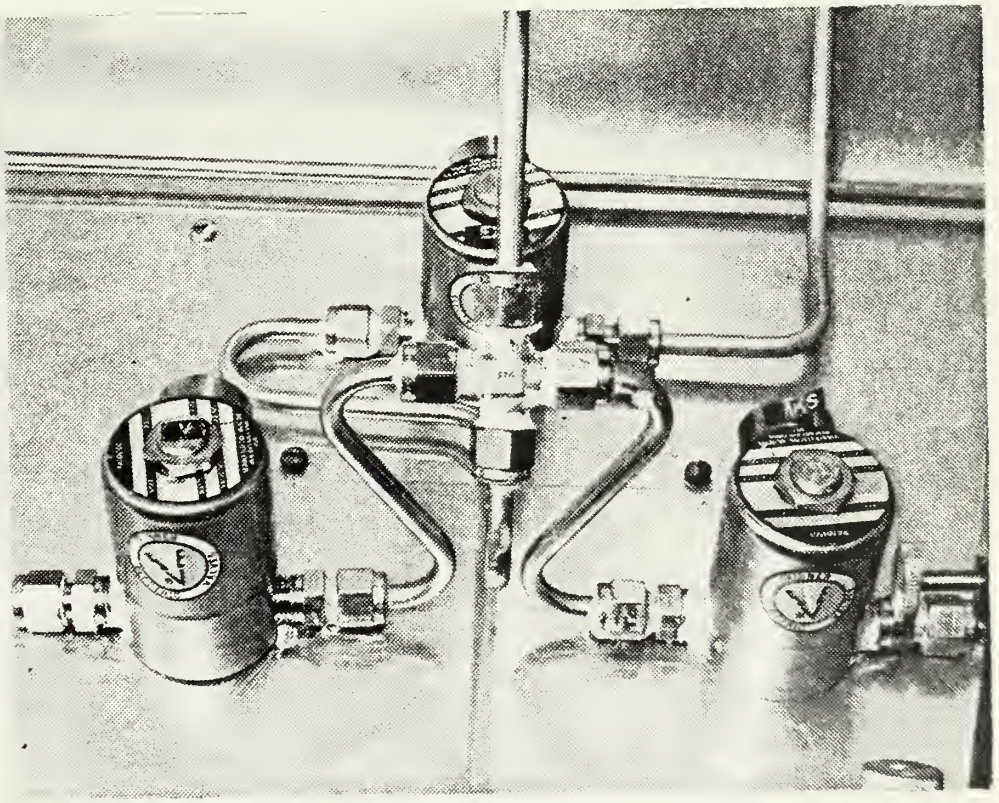

Fig. 5 Skinner Solenoid Valves

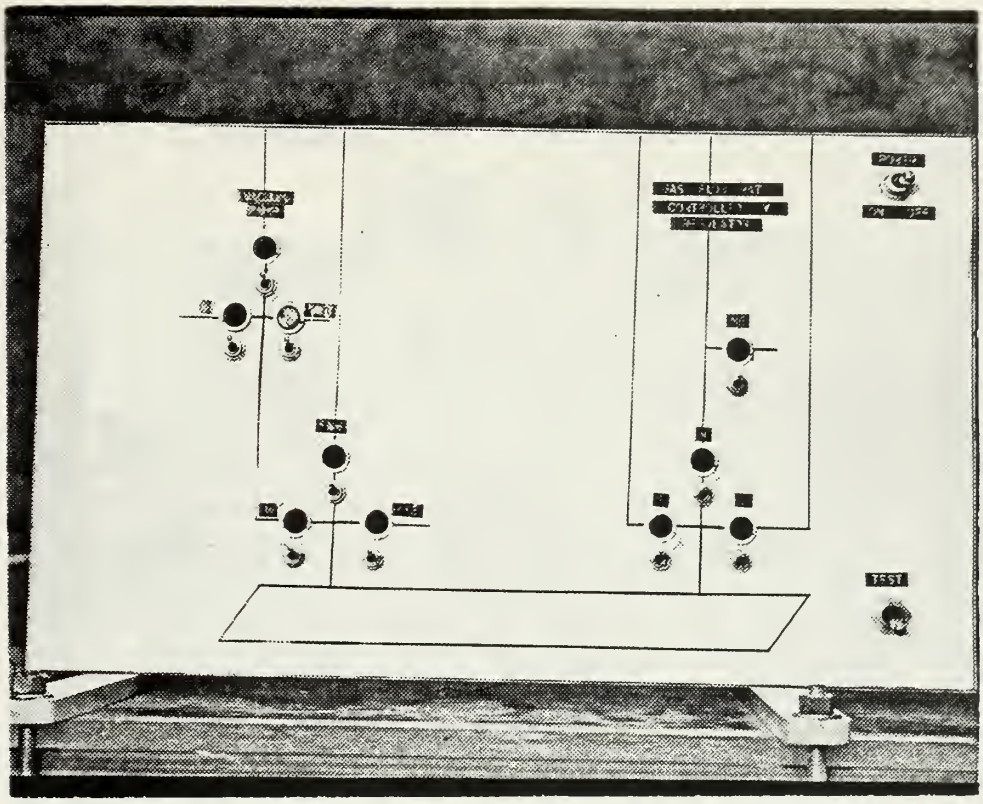

Fig. 4 Gas/Vacuum Valve Control Panel

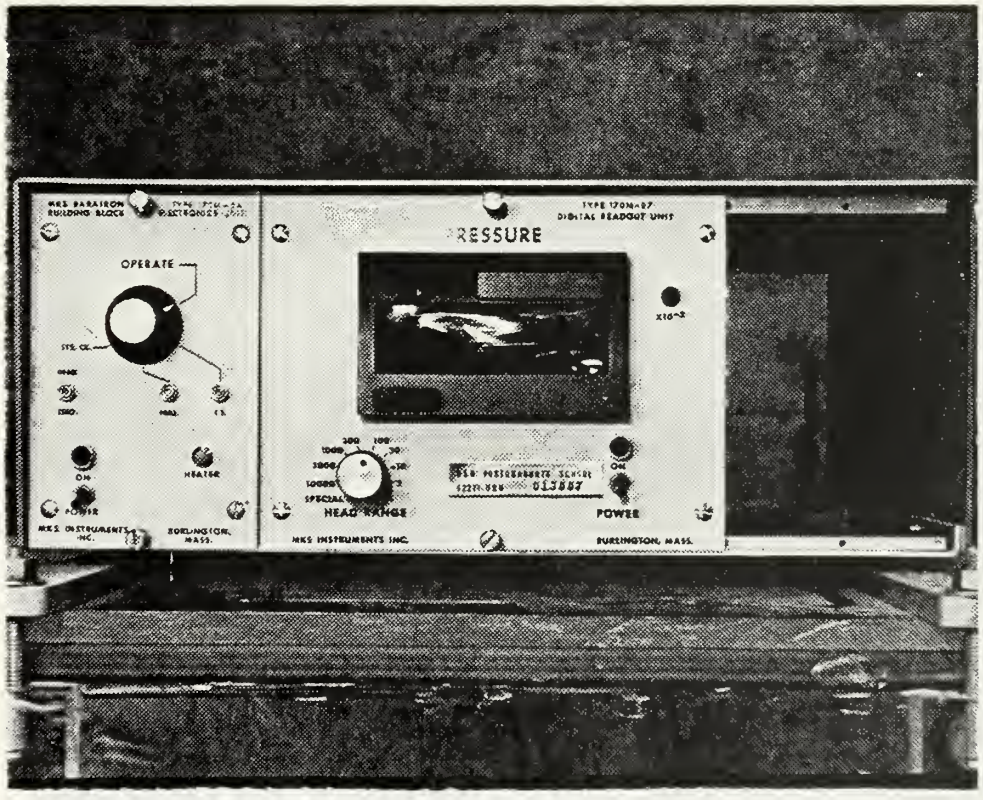

Fig. 7 Baratron-170 Pressure Readout Unit

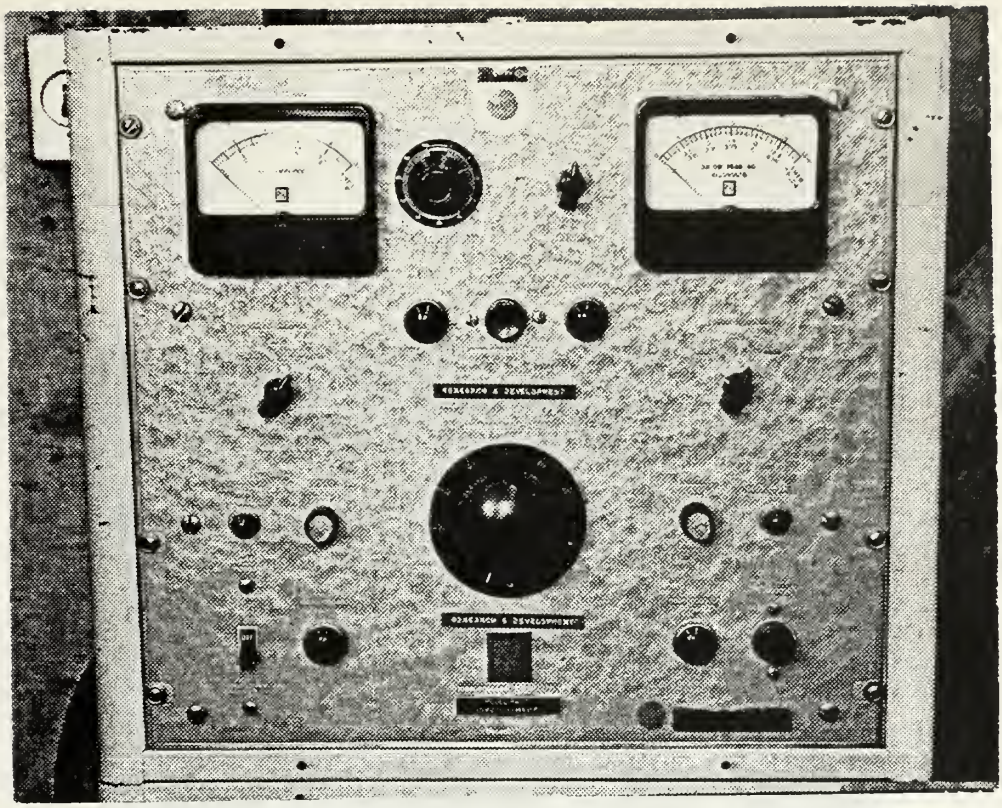

Fig. 8 HA-51 Variable Power Supply

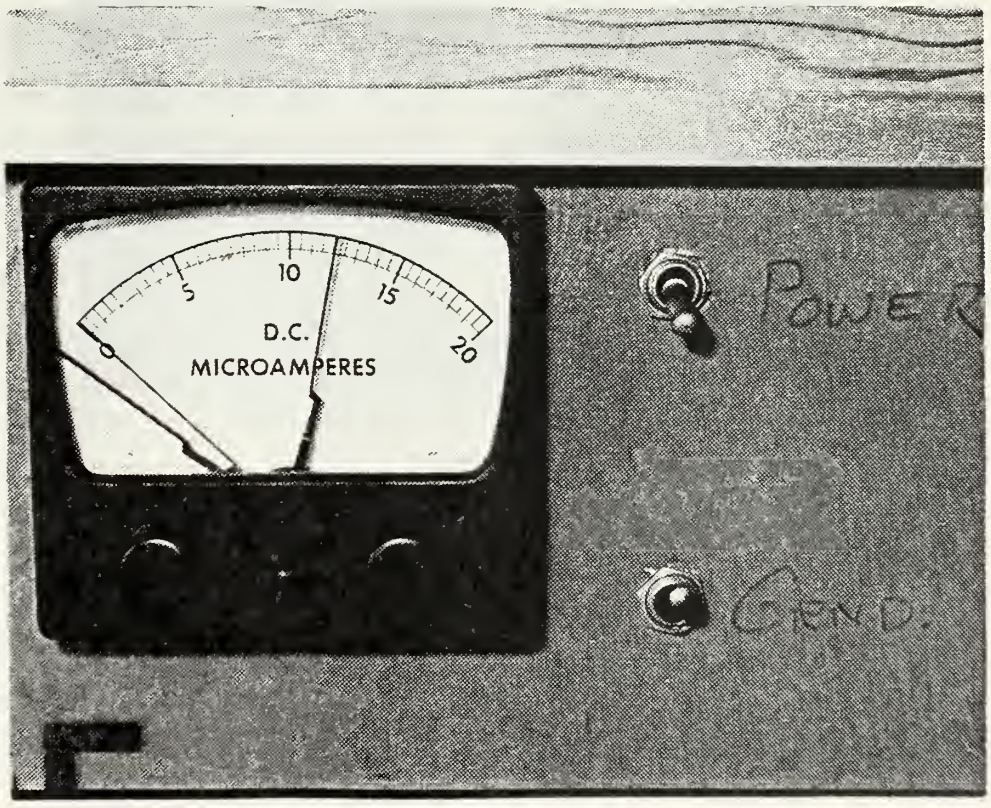

Fig. 9 High Voltage Selection Meter

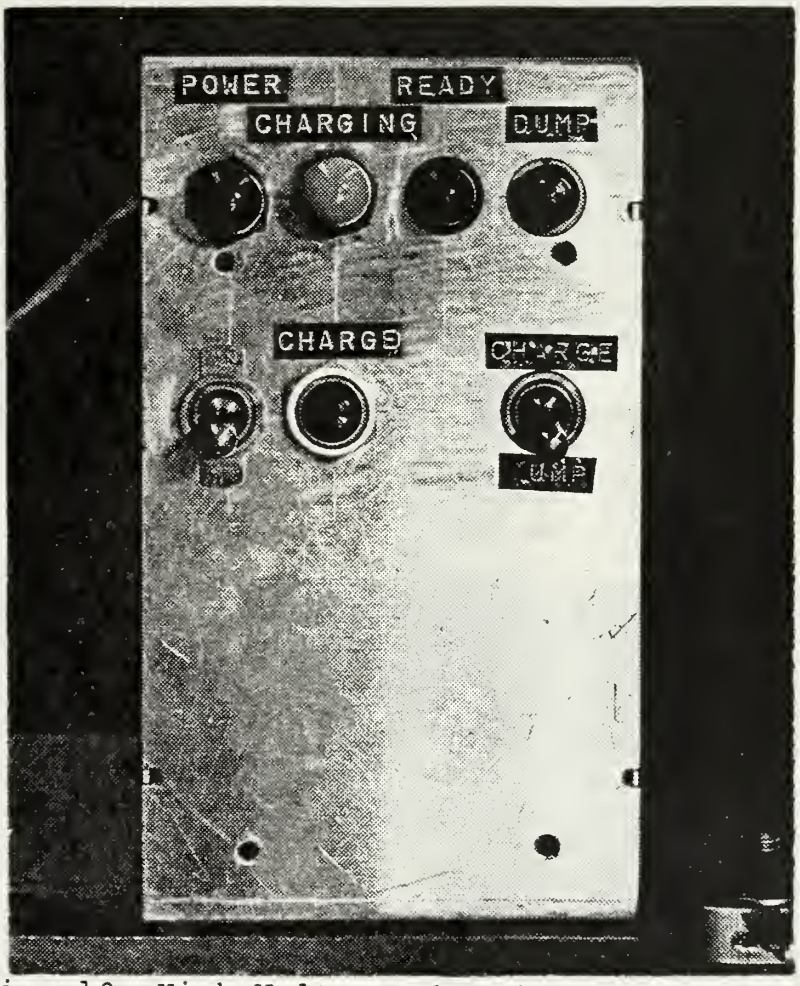

Fig. 10 High Voltage Charging Control Box

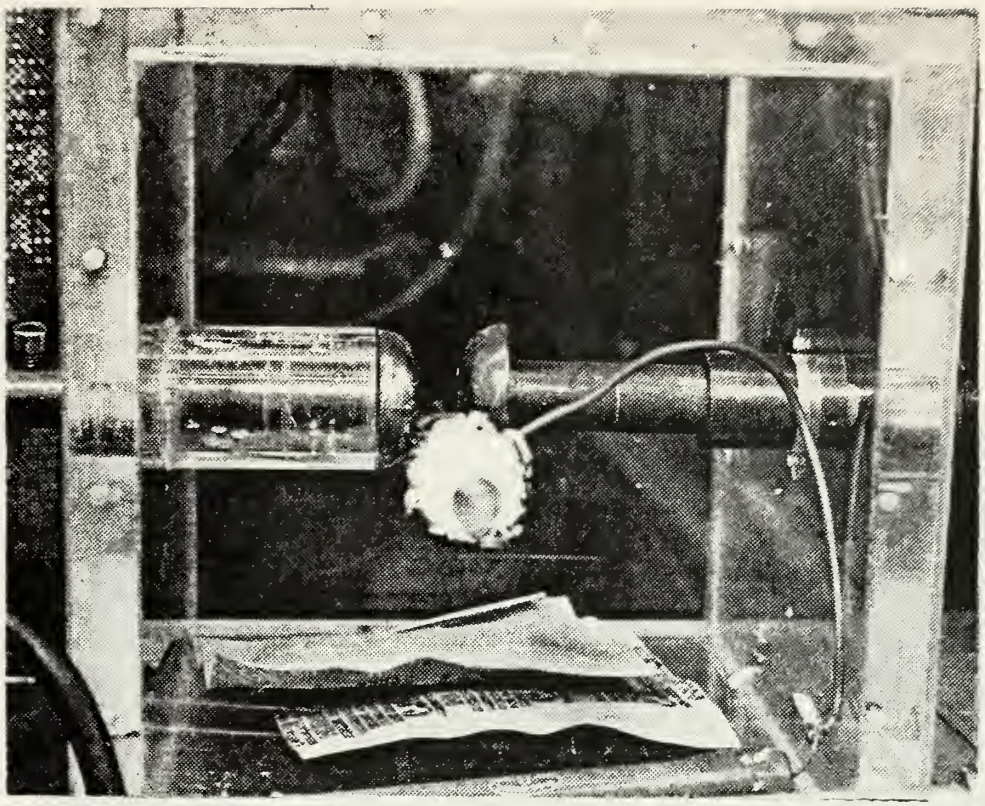

Fig. 11 Spark Gap Enclosure and Copper Electrodes

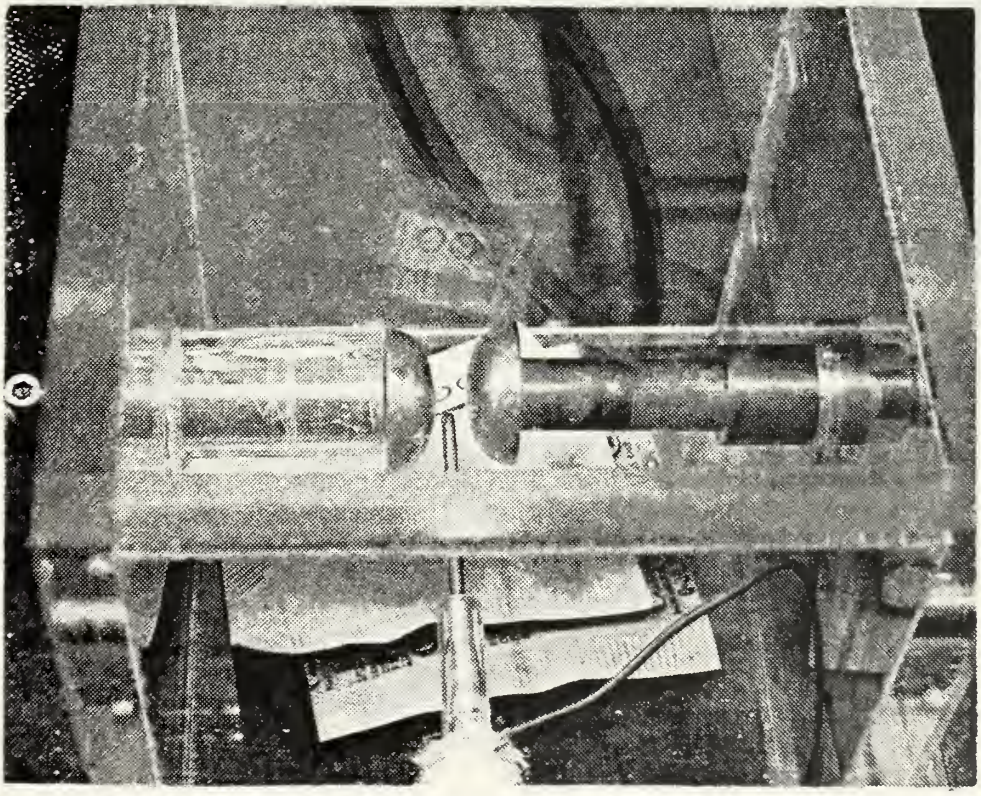

Fig. 12 Spark Gap Assembly Showing Also the Tungsten Electrode

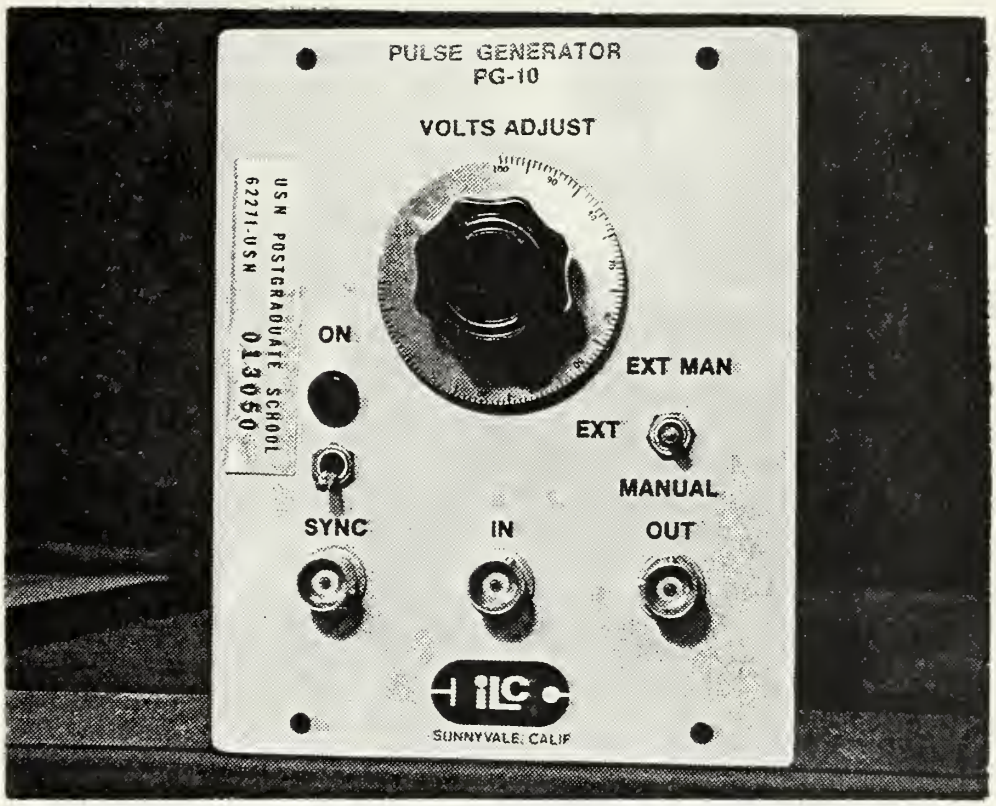

Fig. 13 PG-10 Pulse Generator

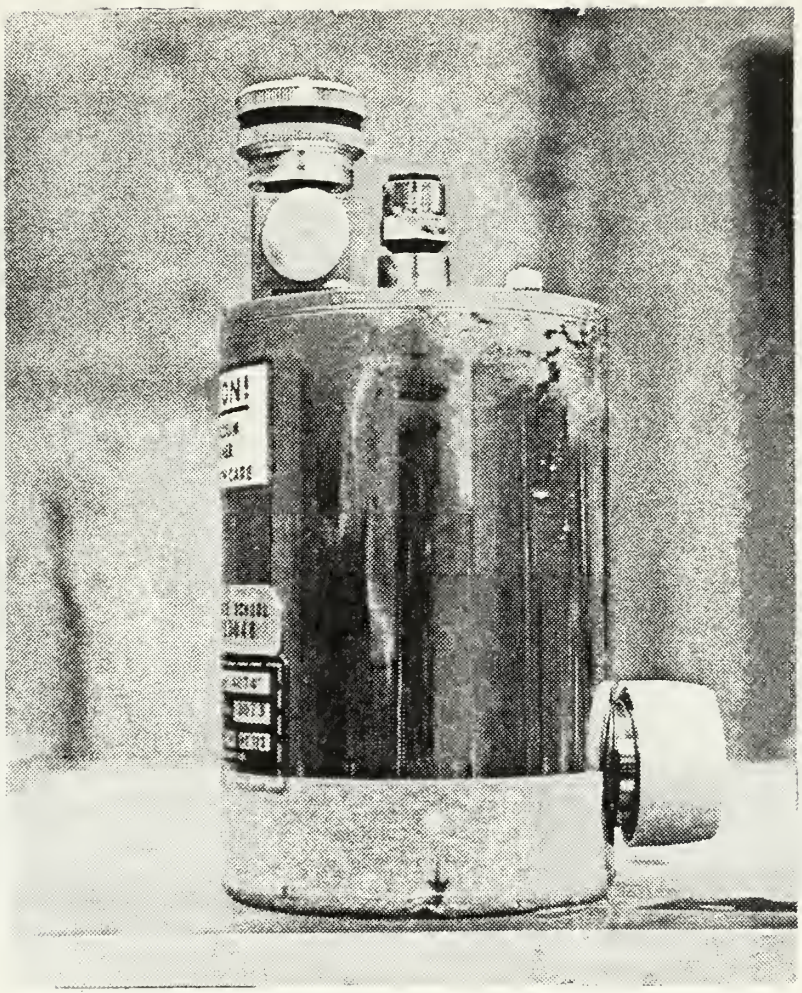

Fig. 14 SBRC Ge:Au IR Detector

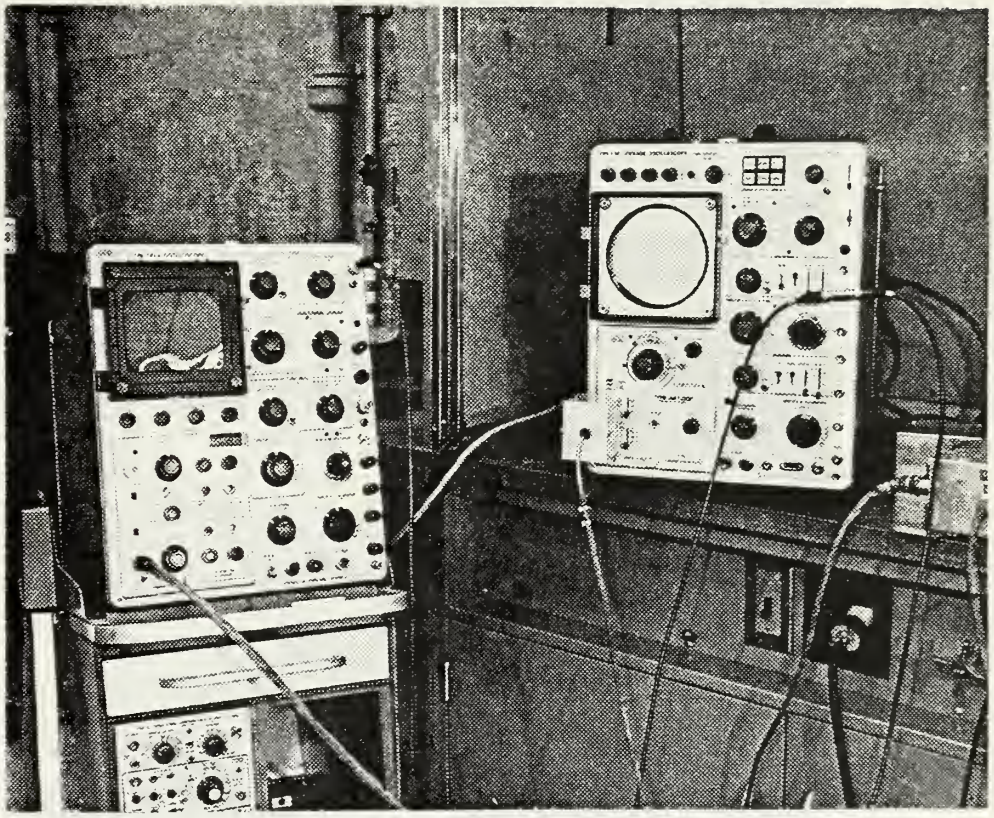

Fig. 15 Oscilloscopes Used to Monitor The Output Radiation

Fig. 16 VE 401 Vacuum Evaporation Unit

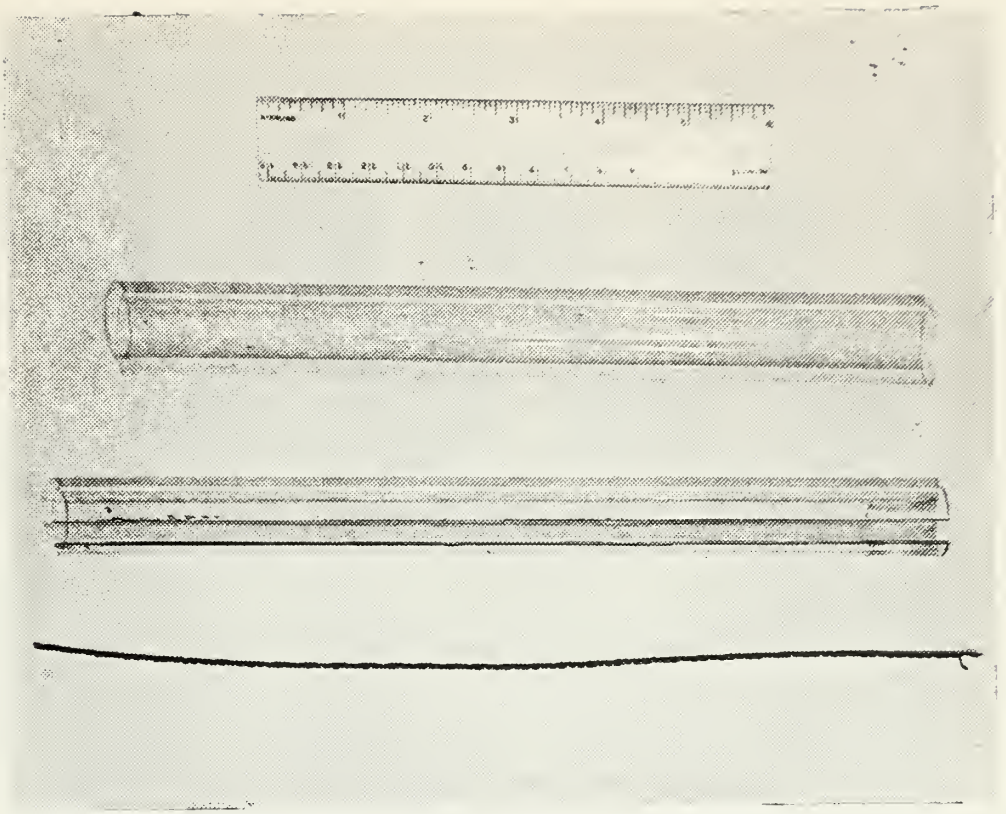

Fig. 17 Disassembled Components of Laser Tube Used In Metal Deposition Process

Fig. 18 The Assembled Components

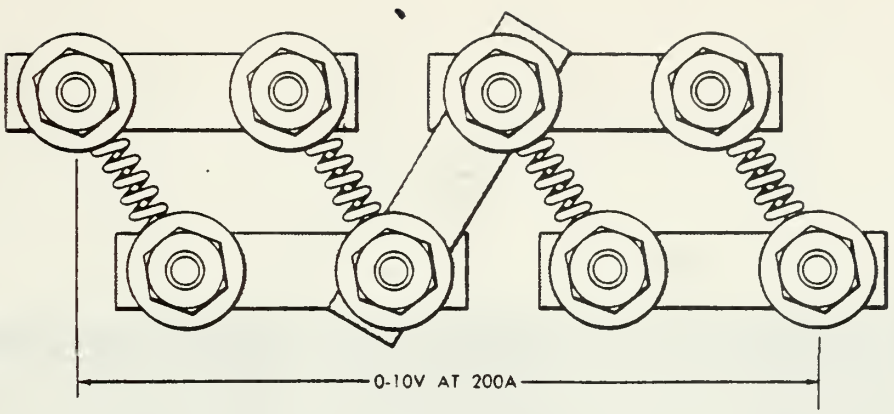

Fig. 19 Bus Bar Arrangement

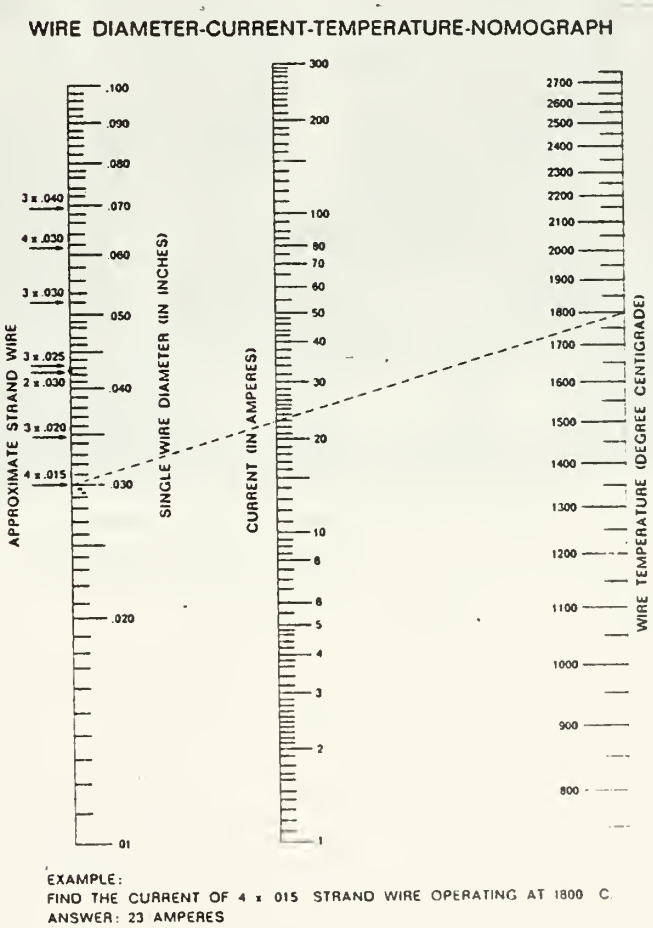

Fig. 20 Current-Temperature Nomograph

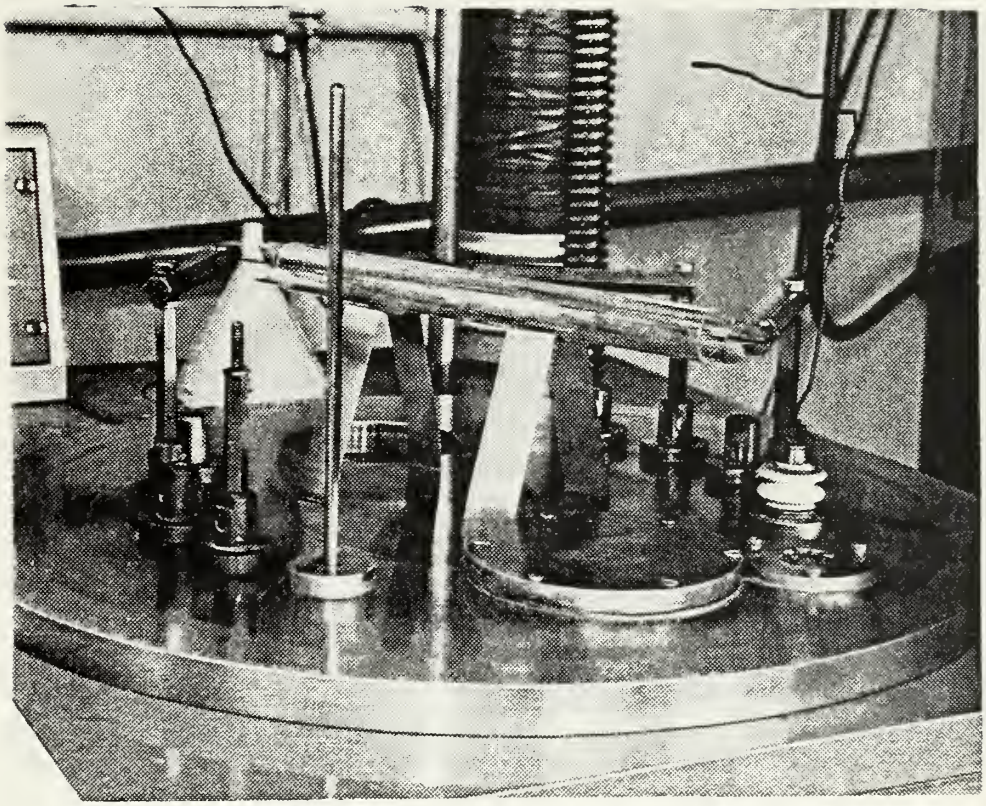

Fig. 21 Assembled Laser Tube Placed in VE 401 Evaporation Unit

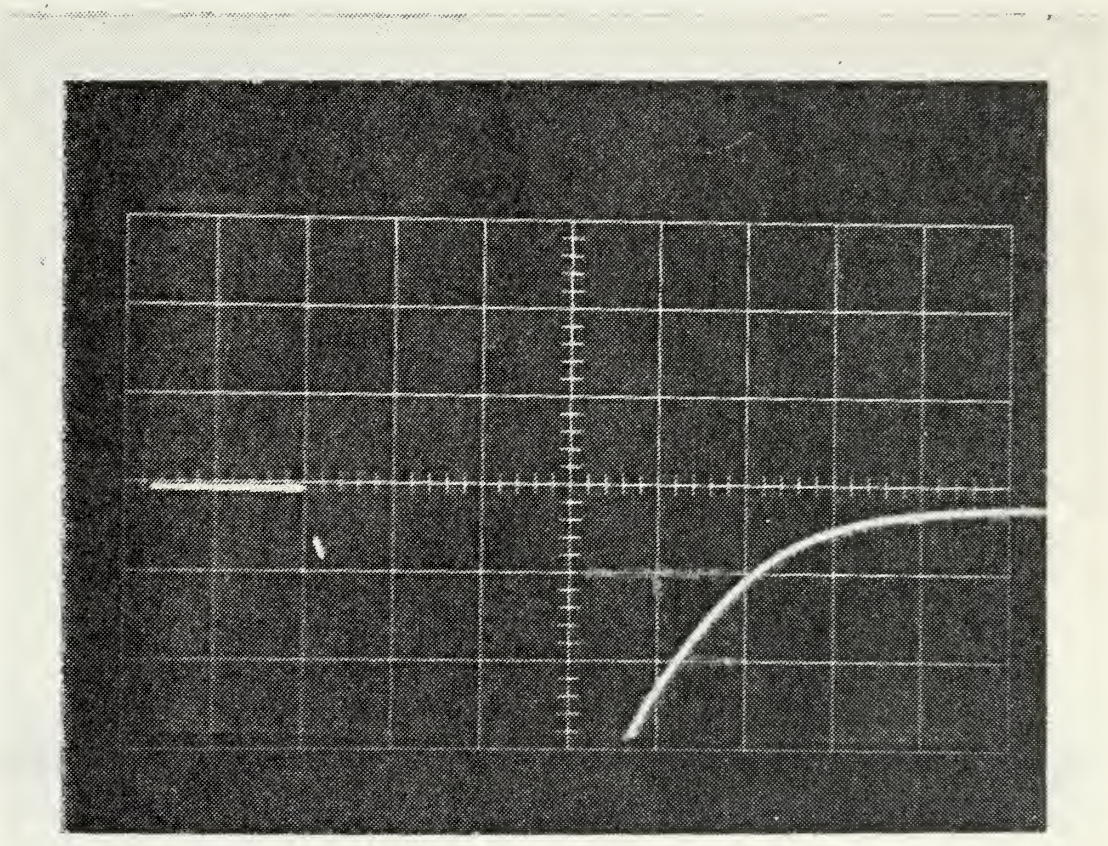

Fig. 22 Experiment I-IR Output
Horizontal Scale 20 microseconds/cm
Vertical Scale 1 Volt/cm

(A)

(B)

Fig. 23 Top(A) and Bottom(B) View Of Laser Tube For Experiment I

(A)

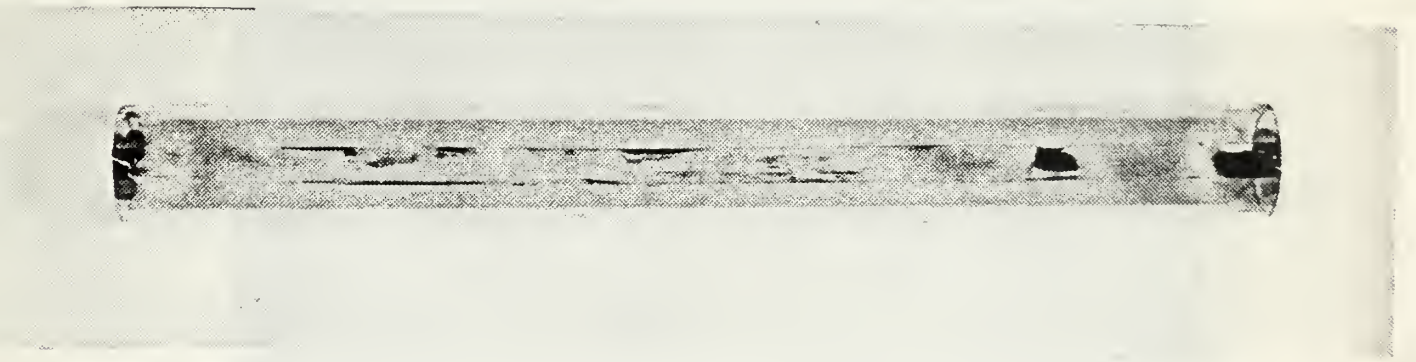

(B)

Fig. 24 Top(A) and Bottom(B) View Of Laser Tube Experiment III

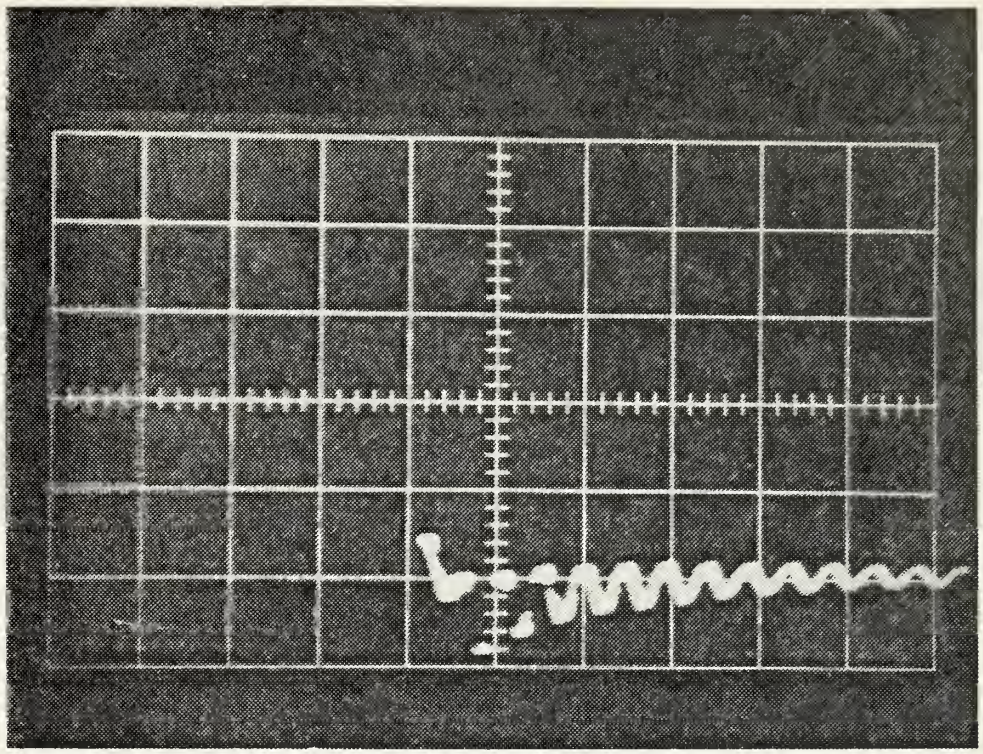

Fig. 25 Experiment III-IR Output
Horizontal Scale 20 microseconds/cm
Vertical Scale 2 Volts/cm

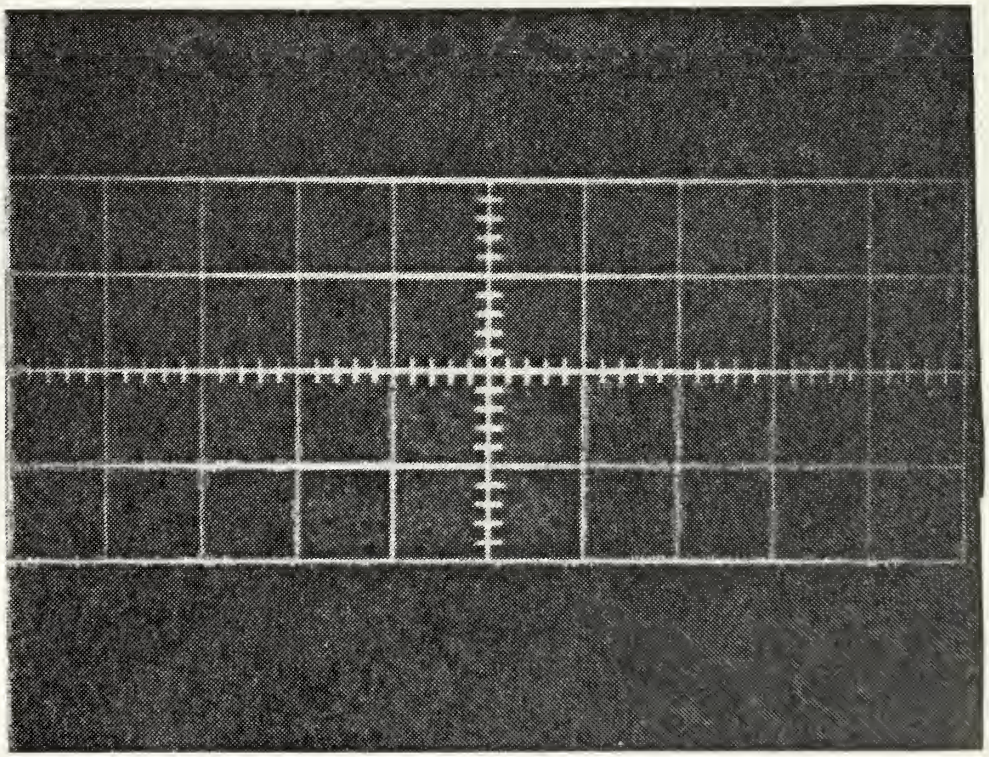

Fig. 26 Experiment III-Photomultiplier Output
Horizontal Scale 20 microseconds/cm
Vertical Scale 2 Volts/cm

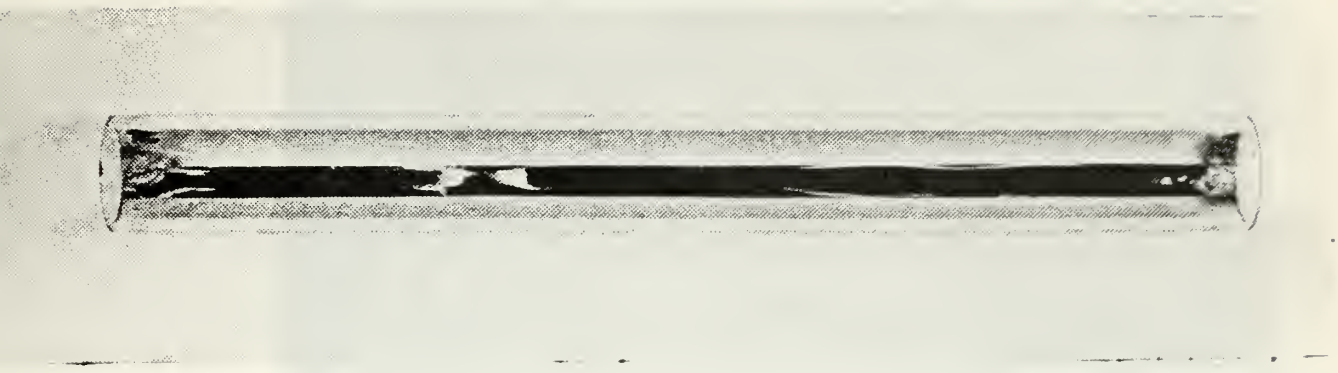

(A)

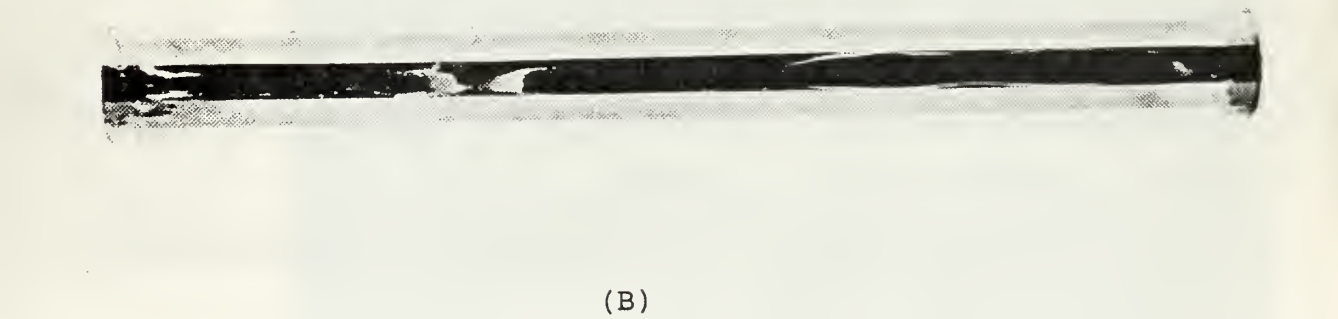

(B)

Fig. 27 Top(A) and Bottom(B) View Of Laser Tube Experiment IV

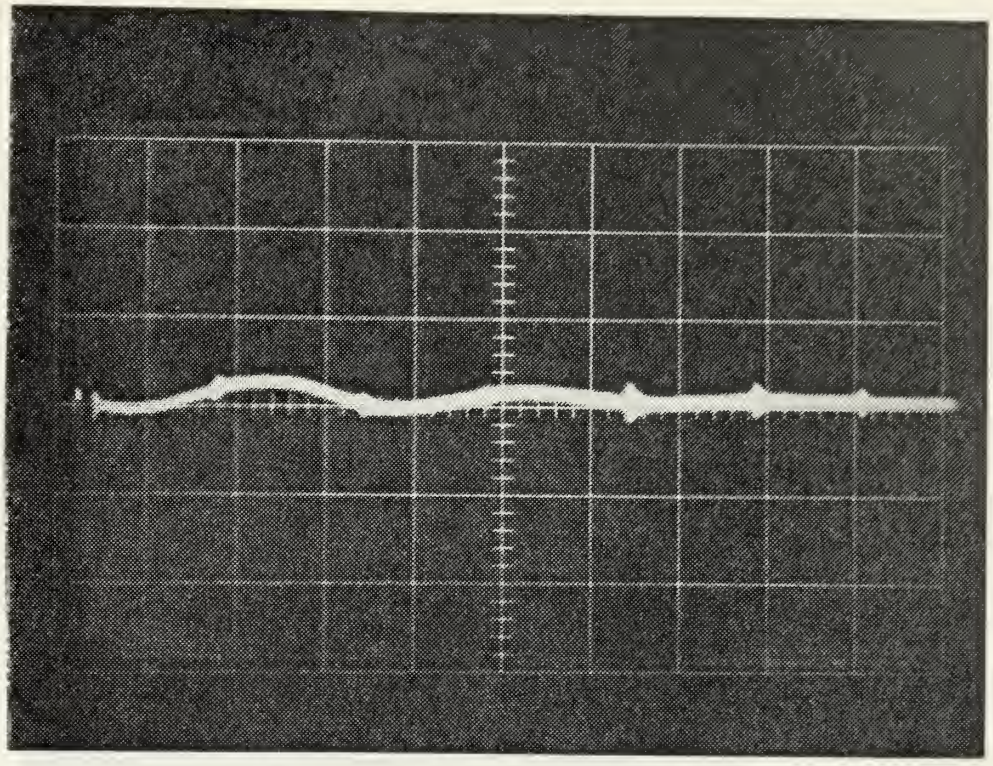

Fig. 28 Experiment IV-IR Output
Horizontal Scale 10 Microseconds/cm
Vertical Scale 5 Volts/cm

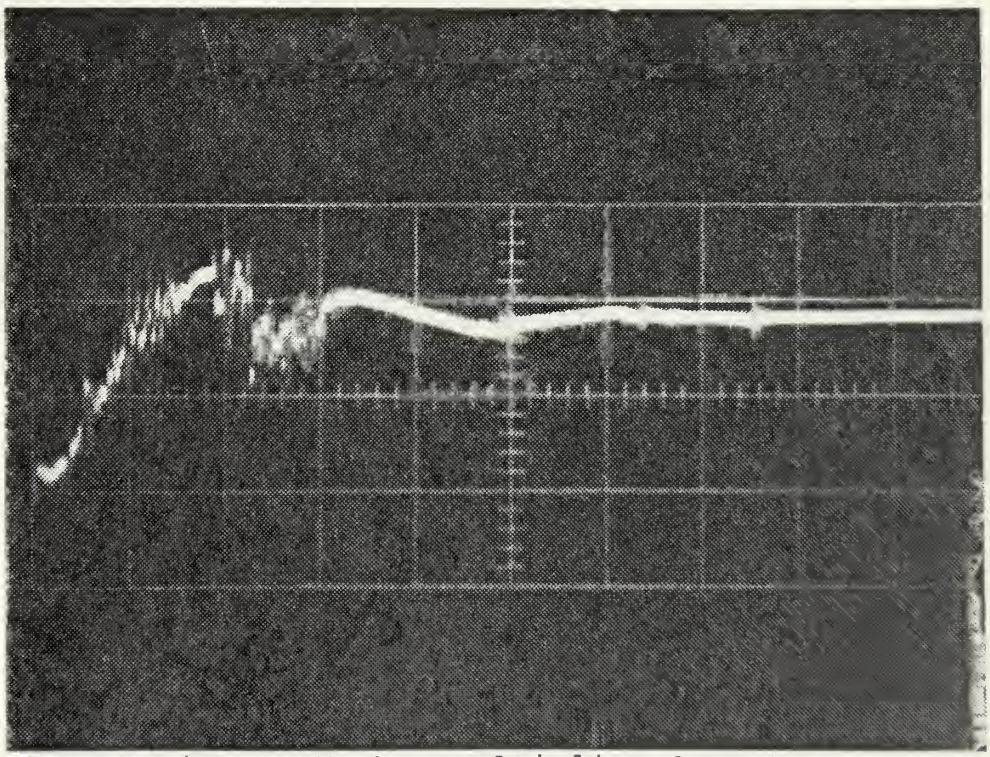

Fig. 29 Experiment IV-Photomultiplier Output
Horizontal Scale 10 Microseconds/cm
Vertical Scale 10 Volts/cm

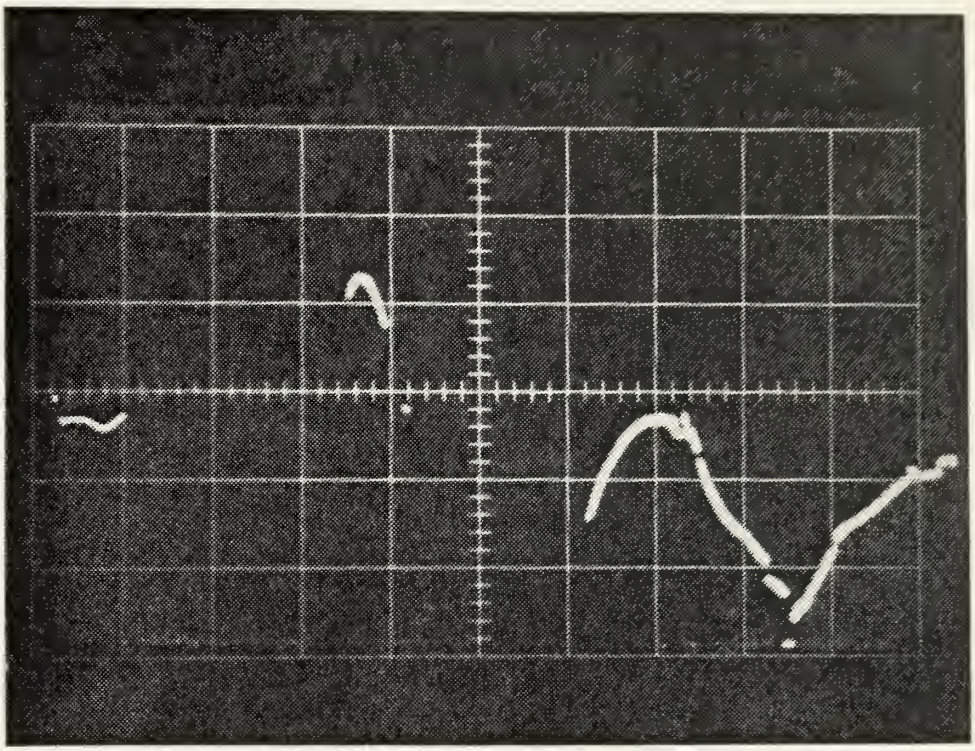

Fig. 30 Experiment V-IR Output
Horizontal Scale 10 Microseconds/cm
Vertical Scale 5 Volts/cm

Fig. 31 Experiment V-Photomultiplier Output
Horizontal Scale 10 Microseconds/cm
Vertical Scale 5 Volts/cm

(A)

(B)

Fig. 32 Top(A) and Bottom(B) View Of Laser Tube After Firing Experiment V

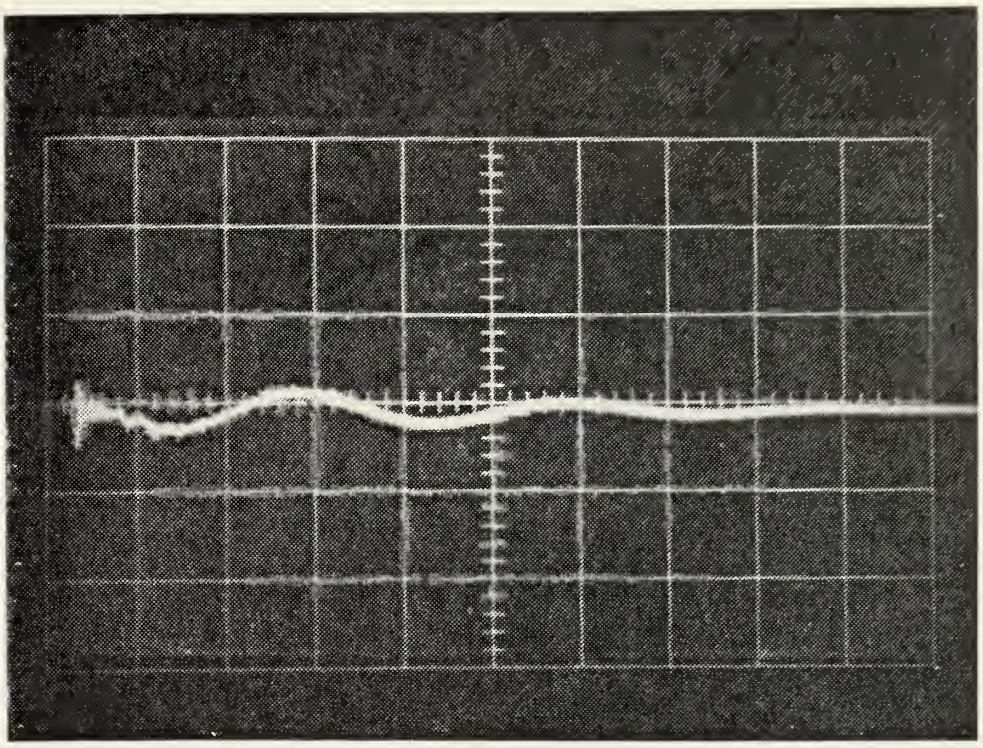

Fig. 33 Experiment VII-IR Output
Horizontal Scale 10 Microseconds/cm
Vertical Scale 5 Volts/cm

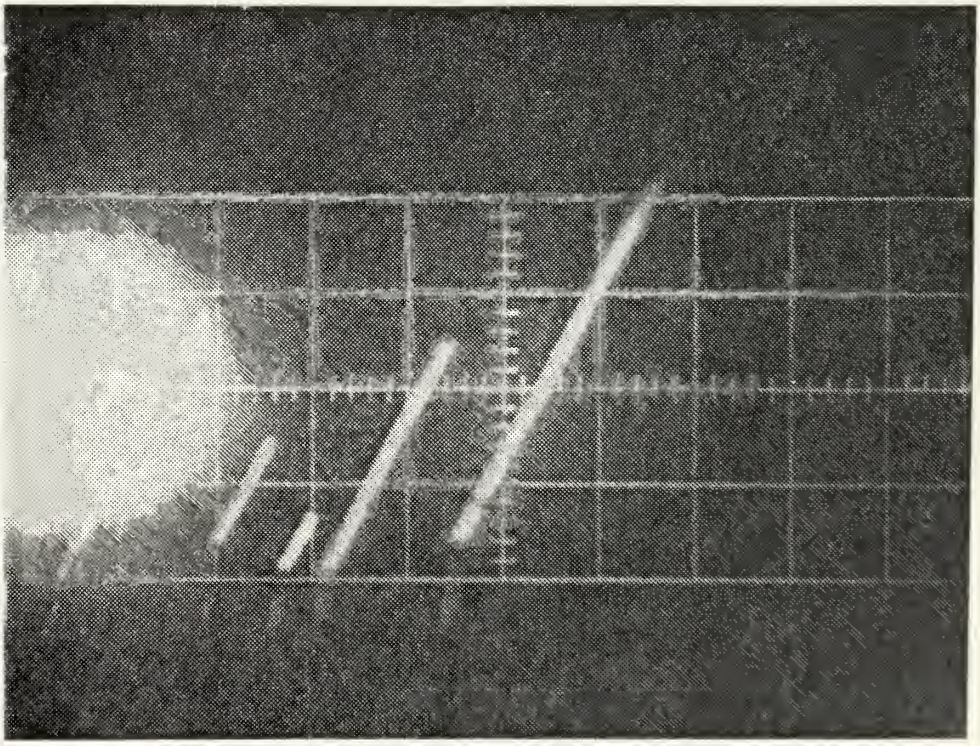

Fig. 34 Experiment VII-Photomultiplier Output
Horizontal Scale 10 Microseconds/cm
Vertical Scale 5 Volts/cm

(A)

(B)

Fig. 35 Top(A) and Bottom(B) View of Laser Tube After Firing Experiment VII

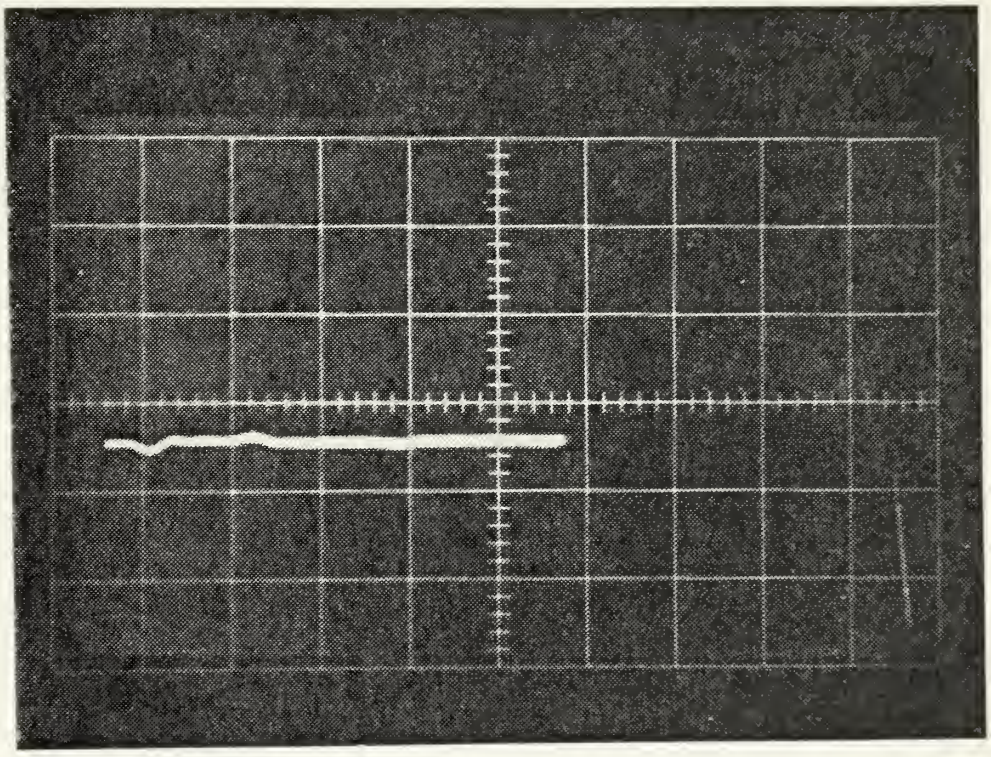

Fig. 36 Experiment VIII-IR Output
Horizontal Scale 10 Microseconds/cm
Vertical Scale 5 Volts/cm

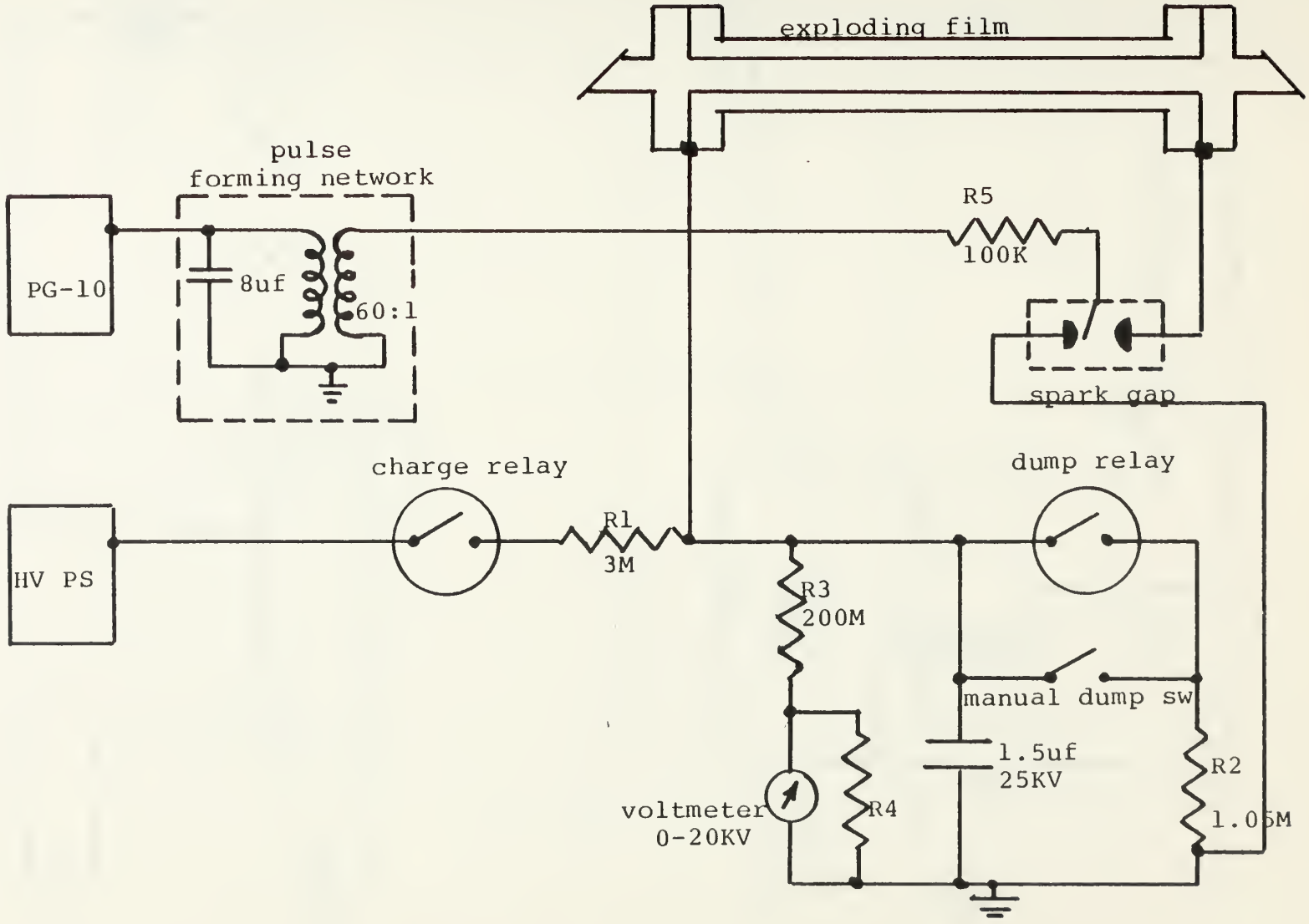

Fig. 37 High Voltage System

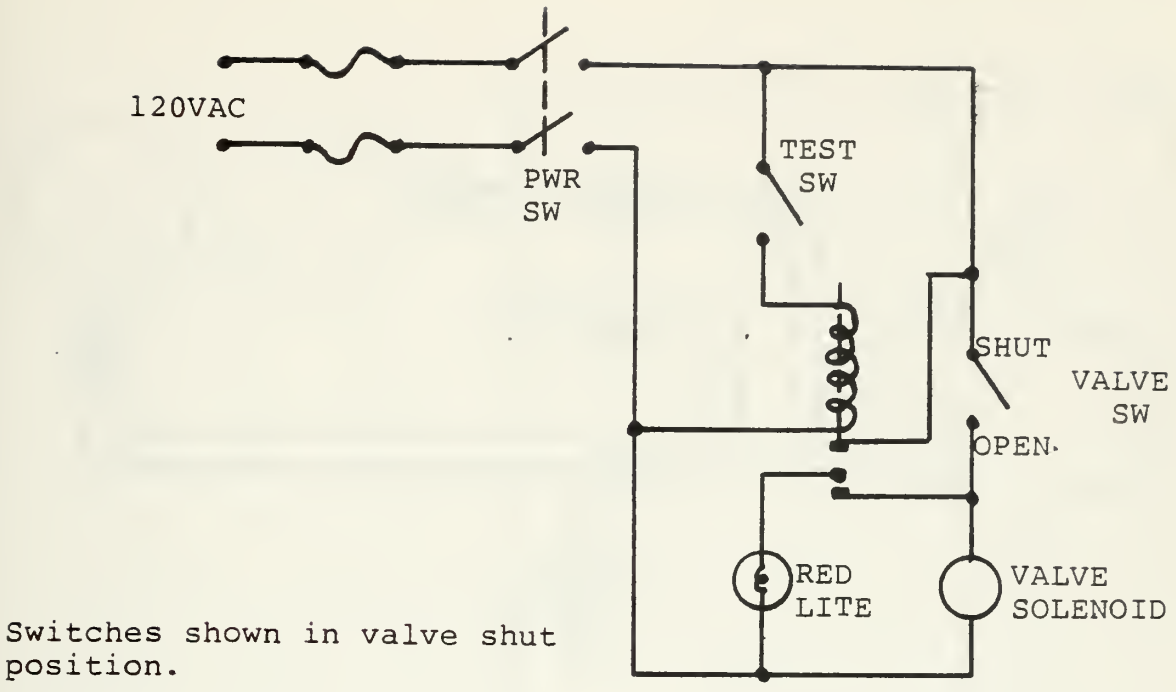

Switches shown in valve shut position.

Fig. 38 Typical Valve Control Circuit

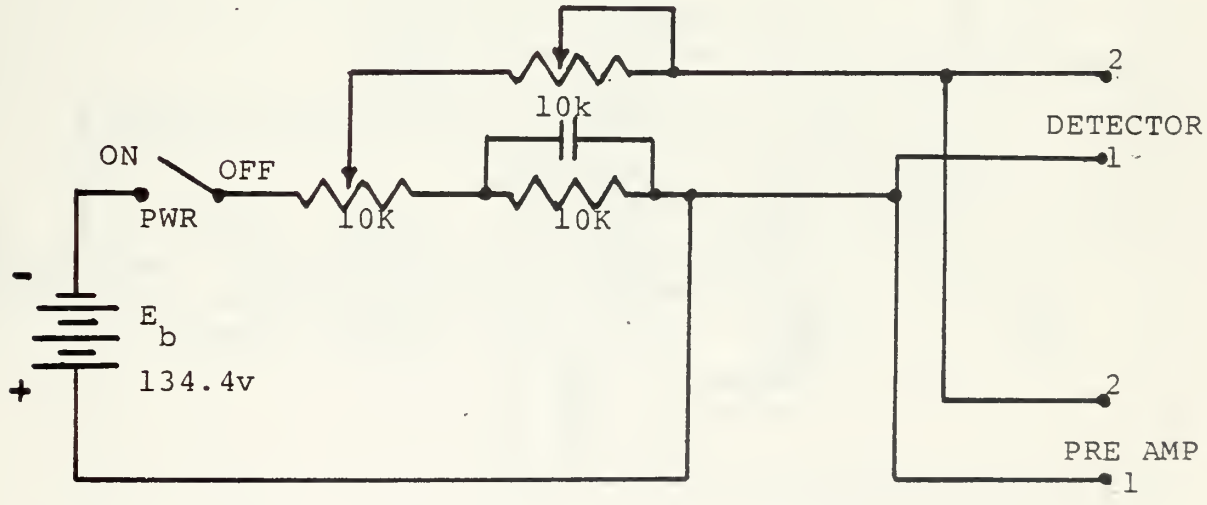

Fig. 39 Detector Bias Circuit

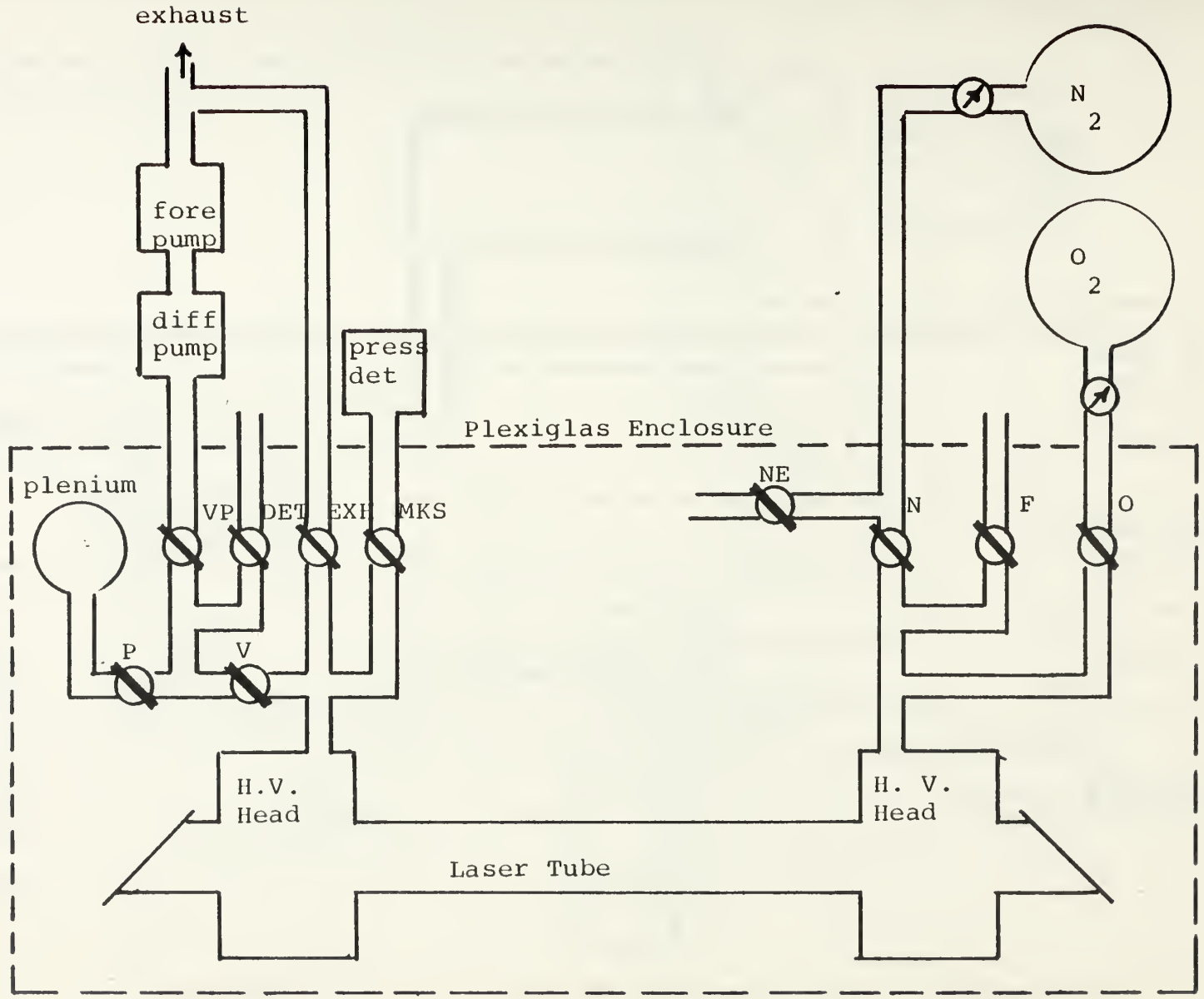

Fig. 40 Vacuum and Gas System

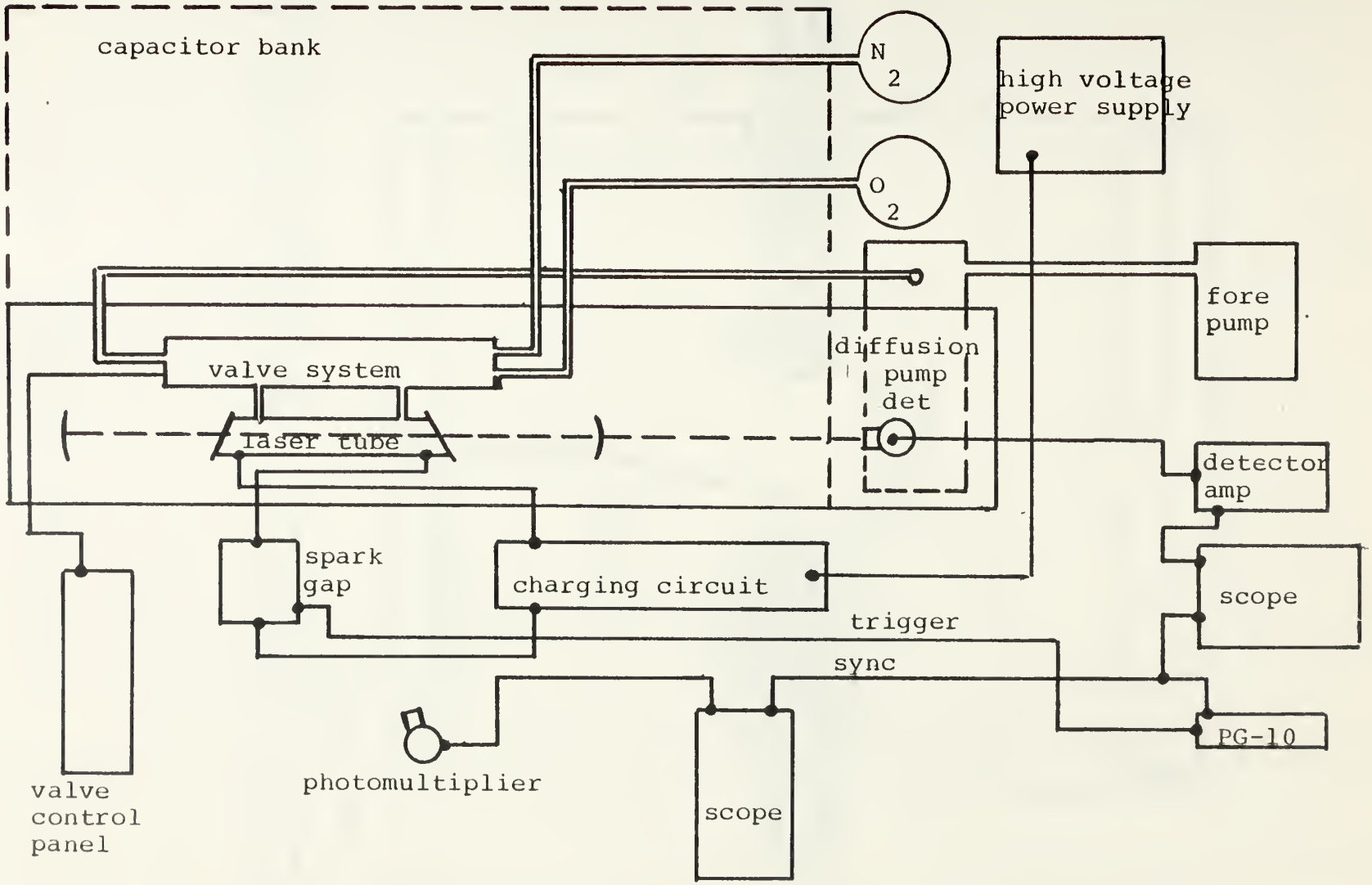

Fig. 41 Experimental Set-up

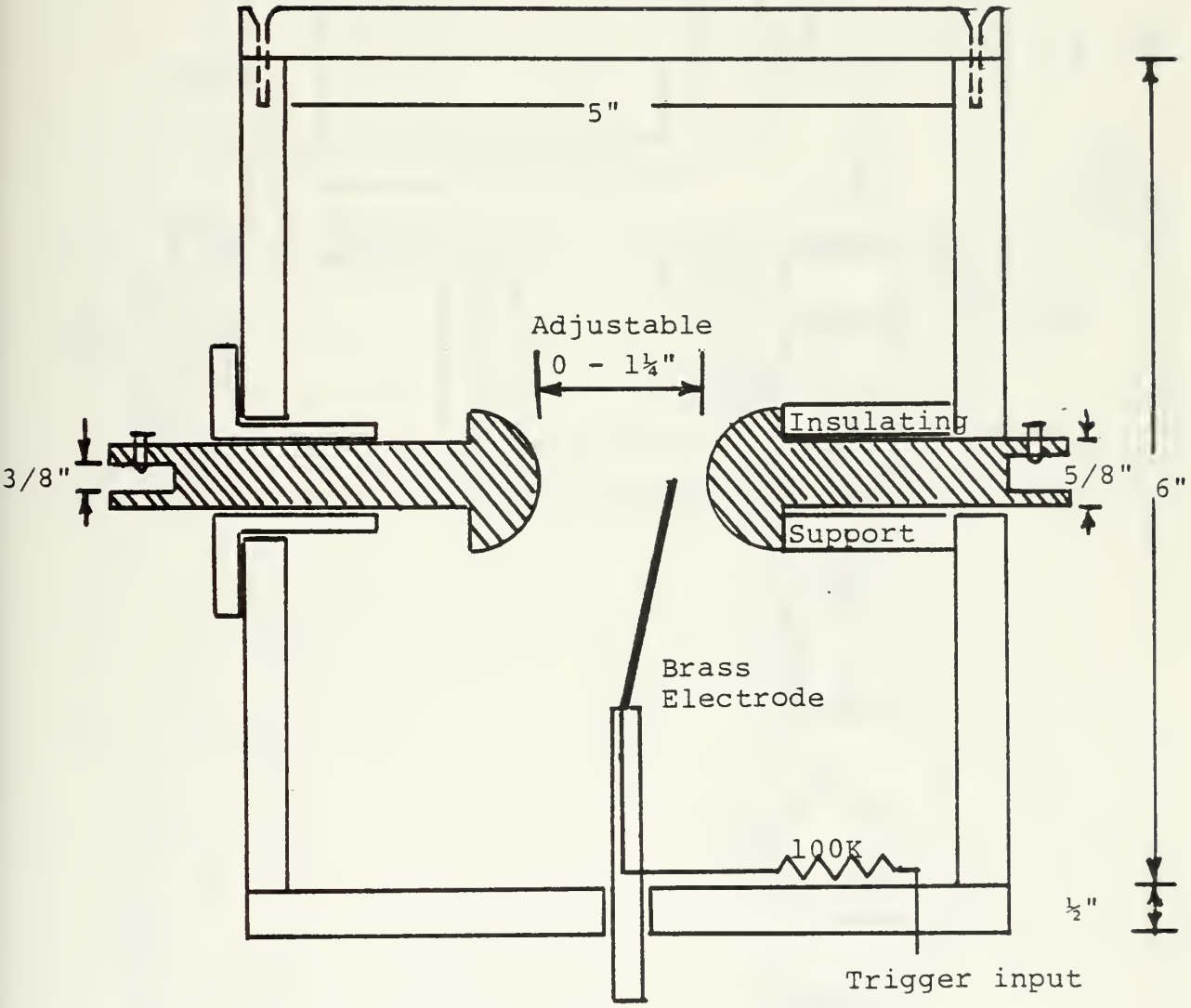

Spark Gap Electrodes are 1¼". Copper hemispheres mounted on 5/8" copper rods. Enclosure and supports are ½" plexiglass.

Fig. 42 Spark Gap Construction

Switch S]: CHARGE/DUMP Switch

All relay and switch contacts shown in charging position.

Note: Modifications not shown on this schematic

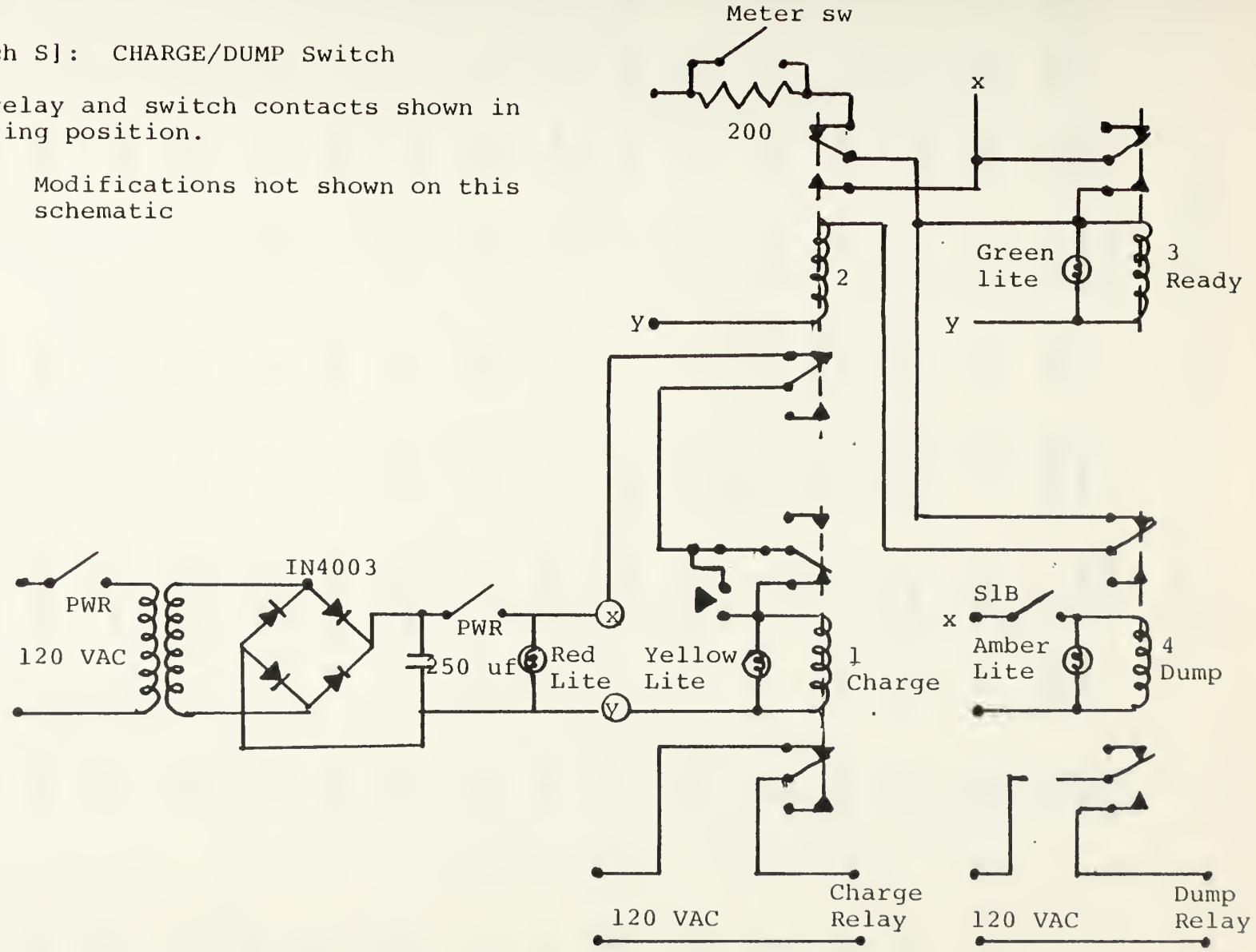

Fig. 43 Charging Control Circuit

PROPERTIES OF RARE EARTH ELEMENTS

Symbol	Atomic No.	Atomic Weight	Estimated Abundance, ppm	Density, g/cm^3	Atomic Volume, cm^3/g-atom	Melting Point, C	Heat of Fusion, kcal/mole	Boiling Point, C	
Y	39	88.92	28-70	4.472	19.7	~1547	4.1	3027	YTTRIUM
La	57	138.92	5-18	6.162 (Hcp) 6.19 (Fcc)	22.43 22.48	920±5	2.4	4515	LANTHANUM
Ce	58	140.13	20-46	6.78 (Fcc) 6.81 (Hcp)	20.58 20.7	804±5	2.2	3600	CERIUM
Pr	59	140.92	3.5-5.5	6.776 (Hcp) 6.805 (Fcc)	20.79 20.71	935±5	2.4	3450	PRASEODYMIUM
Nd	60	144.27	12-24	7.007	20.5	1024±5	2.6	3300	NEODYMIUM
Pm	61	145			No stable isotopes				PROMETHIUM
Sm	62	150.35	4.5-7	7.540	20.0	1052±5	2.6	1900	SAMARIUM
Eu	63	152.0	0.14-1.1	5.166	29.0	826±10	2.3	1700	EUROPIUM
Gd	64	157.26	4.5-6.4	7.868	19.79	1350±20	3.7	3000	GADOLINIUM
Tb	65	158.93	0.7-1	8.253	19.11	1400-1500	3.9	2800	TERBIUM
Dy	66	162.51	4.5-7.5	8.565	18.97	1475-1500	4.1	2600	DYSPROSIUM
Ho	67	164.94	0.7-1.2	8.799	18.65	1475-1525	4.1	2700	HOLMIUM
Er	68	167.27	2.5-6.5	9.058	18.29	1475-1525	4.1	2600	ERBIUM
Tm	69	168.94	0.2-1	9.318	18.12	1500-1550	4.4	2400	THULIUM
Yb	70	173.04	2.7-8	6.959	24.75	824±5	2.2	1800	YTTERBIUM
Lu	71	174.99	0.8-1.7	9.849	17.96	1650-1750	4.6	3500	LUTETIUM

Table 1

ELEMENT	CURRENT*	VACUUM**	FILAMENT	REMARKS***
Cu	26-32	$3X10^{-7}$ $8X10^{-7}$	W-2X.020 32cm length	Good coating; beads on filament
Dy	65	$1X10^{-6}$	3X.025W 3 cin long	1. Not completely evaporated 2. Black Color 3. Sparks when exposed to atmosphere
Eb	70	$2X10^{-6}$	3X.025W 3 cin long	1. Not completely evaporated 2. Black Color 3. Test
Gb	10	$8X10^{-6}$	3X.025W 32 cm long	Test
Ho	70	$2X10^{-6}$	3X.025W 3 cin long	1. Not completely evaporated 2. Black Color 3. Test

* AMPS ** TORR *** SUBSTRATE was a 22mm I.D Pyrex Tube

Table 2

ELEMENT	CURRENT*	VACUUM**	FILAMENT	REMARKS***
La	40	$6X10^{-6}$	2X.020W 5cm length	1. Rapid oxidation upon exposure to atmos.; possibly pyrophoric; test
La	35	$6X10^{-6}$	W-2X.020 5cm length	1. Rapid oxidation upon exposure to atmos.; possibly pyrophoric; test
Tb	55	$1.2X10^{-6}$	3X.025W 32 cm long	1. Wet filament 2. Satisfactory evaporation 3. Test
Tb(1)	50	$.2X10^{-6}$	3X.025W 32 cm long	1. Filament touching inside surface, poor center deposit
Tb(2)	50	$2X10^{-6}$	3X.025W 32 cm long	1. Touching, but more current allowed to compensate for loss of heating (tube cracked)

* AMPS ** TORR *** SUBSTRATE was a 22mm I.D Pyrex Tube

ELEMENT	CURRENT*	VACUUM**	FILAMENT	REMARKS***
Tb(3)	44	$2X10^{-6}$	3X.025W 32 cm long	1. Ceramic beads on fila. 2. Good strip
Tb(4.5)	44-50	$2X10^{-6}$ $4X10^{-6}$	3X.025W 32 cm long	1. Cracked laser and slotted tubes 2. Repeat deposition 3. Cracked second slotted tube
Tb(6,7)	42	$1X10^{-6}$	3X.025W 32 cm long	1. Coated entire inside of laser tube 2. Two laser tubes made
Tb(8)	48	$1X10^{-6}$	3X.025W 32 cm long	1. Cracked tube; caused by ceramic bead hot spot
W	100	$9X10^{-7}$	3X.025W 3 cin long	1. No coating 2. Bright Glow 3. Test

* AMPS ** TORR *** SUBSTRATE was a 22mm I.D Pyrex tube

ELEMENT	TEMP (C)	EVAP. RATE
Dy	1128	$1.99X10^{-4}$
Nd	1345	$1.74X10^{-4}$
Pr	1429	$1.68X10^{-4}$
La	1740	$1.53X10^{-4}$

(g/cm^2-sec)

Table 3

Evaporation Temperatures and Rates of Evaporation [13]

[13] Powell, Oxley, Blocher, Vapor Deposition, p. 224-225

MONOXIDE	$-H_{f\ 0}$ (KCAL/MOLE)
LaO	31.3
NdO	36.9
PrO	33.3
SmO	34.5
TbO	20.0
DyO	20.1
GdO	17.8
HoO	23.8
ErO	17.1
YbO	-7.2

Table 4

Heats of Formation for Gaseous Rare Earth Monoxides [14]

[14] Ames, L. L., Walsh, P. N., White, D., "Dissociation Energies of the Gaseous Rare Earths", Journal of Physical Chemistry, Vol 71, Number 8, p. 2714, July 1967

APPENDIX C

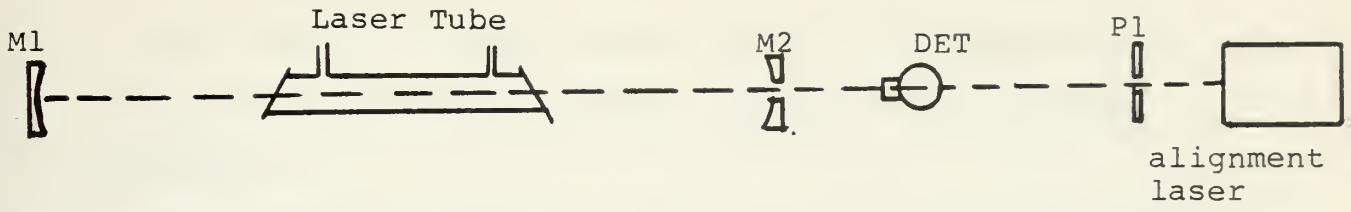

ALIGNMENT

Following are steps used in the alignment of the laser optical cavity:

1. Direct laser beam (He-Ne) through both NaCl windows so that it is centered as nearly as possible.

2. Adjust Mirror 1 (M1) so that laser beam impinges directly at the center.

3. Place pin hole (P1) on the optical bench and adjust height for maximum output through pin hole.

4. Adjust M1 so that the reflected beam strikes the pin hole.

5. Place the output Mirror (M2) on the optical bench and adjust for maximum output.

6. Readjust M1 so that reflected beam impinges directly on the hole in M2.

7. Adjust M2 to put its reflection on the center of M1.

8. Place IR detector pedestal on the optical bench (be sure it is level)

9. Place detector on pedestal so that it is facing the laser.

10. Raise or lower pedestal until laser beam enters the detector directly centered. Remove detector when completed.

11. Suspend plumb-bob from the top of the plexiglass enclosure and move it until laser beam strikes the string.

12. Repeat 11 for opposite side of the pedestal (this will hopefully give a direct line of sight from the detector along the longitudinal axis of the optical cavity).

13. Mark the base of the detector (front and rear) such that the detector entrance window is as nearly perpendicular to the longitudinal axis as possible.

14. Place detector on the pedestal with window facing M2. (be sure marks on pedestal and those on detector are in line.)

15. System is aligned; remove alignment laser.

EQUIPMENT

1. One small He-Ne or similar laser
2. One adjustable triped
3. One level
4. One plumb-bob
5. Two three-degree of freedom mounts
6. Two 10-meter radii gold surfaced mirrors (one with 1 mm output coupling hole)

7. One pin-hole (about 2 mm hole.)
8. One detector pedestal
9. One detector

APPENDIX D - FIRING PROCEDURE

The following is a step-by-step procedure that was used to vaporize the metallic film once the laser tube was placed between the high voltage heads and electrical connections made:

1. Check high voltage rheostat on HA-51 power supply is set at zero (no power otherwise).
2. Turn on HA-51 power supply (green lite on)
3. Push HA-51 high voltage start button (green lite, out, red lite on)
4. Pull manual grounding plug on top of plywood enclosure
5. Select desired voltage
6. Turn charging system on (top switch next to high voltage selection meter)
7. Turn HA-51 power stat to approximately 40
8. Check charge-dump switch on portable charging box in the dump position
9. Place portable charging box power switch to on (amber lite on)
10. Select desired pressure
11. Charge-dump switch to charge (amber lite out)
12. Punch charge button (yellow lite on)
13. Green lite on when charging complete
14. Depress manual trigger on PG-10 box to fire

To Dump

1. Turn HA-51 high voltage rheostat to zero

2. Depress primary dump switch (momentary toggle switch next to high voltage selection meter and below charging circuit switch)

3. Portable control box charge-dump switch to dump (amber lite on)

4. Portable control box on-off switch to off to extinguish ready lite may be turned on as desired

```
REM DIATOMIC MOLECULAR SPECTRA
READ A,B
READ C,D
DIM Y(10,10)
FOR M=0 TO D
FOR L=0 TO C
READ Y(L+1,M+1)
NEXT L
NEXT M
FOR V=1 TO A
PRINT 'V=',V,'TO', V-1,'P- AND R-BRANCH TRANSITIONS FOR',
PRINT'GADOLINIUM OXIDE'
PRINT 'J OF P(J)','WAVE NO.','WAVELENGTH','J OF R(J)',
PRINT 'WAVE NO.','WAVELENGTH'
FOR J=1 TO B
LET I=J-1
LET S1=0
LET S2=0
LET G=0
FOR L=0 TO C
LET G=G+Y(L+1,1)*((V+.5)**L-(V-.5)**L)
NEXT L
FOR L=0 TO C
FOR M=1 TO D
LET R=Y(L+1,M+1)
LET E=(V+.5)**L*(I+1)**M*(I+2)**M
LET S1=S1+R*((V+.5)**L*J**M*(J-1)**M-(V-.5)**L*J**M*(J+1)**M)
LET F=(V-.5)**L*I**M*(I+1)**M
LET S2=S2+R*(E-F)
NEXT M
NEXT L
LET       S1=S1+G
LET S2=S2+G
PRINT J,S1,10000/S1,I,S2,10000/S2
NEXT J
PRINT
PRINT
PRINT
PRINT
NEXT V
DATA 10,25
DATA 3,1
DATA 0.0,841.0,-3.7,0.0
DATA 0.C,0.0,0.0,0.0
END
```

APPENDIX E

DIATOMIC MOLECULAR SPECTRA CALCULATIONS

Included in Ref. 2 is a computer program written in basic language to determine the wave number and wave length for the P- and R- branch transitions ($\Delta\nu = 1$) for a number of diatomic molecules.

This program was used to find the wave number and wave length for the P- and R- branch transitions for GdO, LaO, and PrO. The constants used in the calculations for GdO and PrO were found in Ref. 7 and apply to the "X" (ground state). The constants for LaO came from Ref. 8 and also apply to the "X" state, no other constants were found for the remaining seven rare earth diatomic molecules.

The constants were assembled in matrix format according to the following assumptions:

$\omega_e \sim Y_{10}$ $\quad B_e \sim Y_{01}$ $\quad D_e \sim -Y_{02}$ $\quad \omega_e y_e \sim Y_{30}$ $\quad \gamma_e \sim Y_{21}$

$\omega_e x_e \sim -Y_{20}$ $\quad \alpha_e \sim -Y_{11}$ $\quad \beta_e \sim -Y_{12}$ $\quad \omega_e z_e \sim -Y_{40}$

$\delta_e \sim -Y_{31}$

The Matrix therefore became:

$$\begin{matrix} Y_{00} & Y_{10} & Y_{20} & Y_{30} & \cdots & Y_{0} \\ Y_{01} & Y_{11} & Y_{21} & Y_{31} & \cdots & Y_{1} \\ \vdots & & & & & \\ Y_{om} & \cdots & \cdots & \cdots & \cdots & Y_{1m} \end{matrix}$$

Zero was used to fill in for unknown constants.

	B_e	D_e	ω_e	$\omega_e x_e$	α_e	β_e	$\omega_e y_e$	$\omega_e z_e$	γ_e	δ_e
GdO			841.0	3.7						
LaO			817.26	3.097			0.0406			
PrO			818.9	1.2						

J OF P(J)	WAVE NO.	WAVELENGTH	J OF R(J)	WAVE NO.	WAVELENGTH
1	833.6	11.9962	0	833.6	11.9962
2	833.6	11.9962	1	833.6	11.9962
3	833.6	11.9962	2	833.6	11.9962
4	833.6	11.9962	3	833.6	11.9962
5	833.6	11.9962	4	833.6	11.9962
6	833.6	11.9962	5	833.6	11.9962
7	833.6	11.9962	6	833.6	11.9962
8	833.6	11.9962	7	833.6	11.9962
9	833.6	11.9962	8	833.6	11.9962
10	833.6	11.9962	9	833.6	11.9962
11	833.6	11.9962	10	833.6	11.9962
12	833.6	11.9962	11	833.6	11.9962
13	833.6	11.9962	12	833.6	11.9962
14	833.6	11.9962	13	833.6	11.9962
15	833.6	11.9962	14	833.6	11.9962
16	833.6	11.9962	15	833.6	11.9962
17	833.6	11.9962	16	833.6	11.9962
18	833.6	11.9962	17	833.6	11.9962
19	833.6	11.9962	18	833.6	11.9962
20	833.6	11.9962	19	833.6	11.9962
21	833.6	11.9962	20	833.6	11.9962
22	833.6	11.9962	21	833.6	11.9962
23	833.6	11.9962	22	833.6	11.9962
24	833.6	11.9962	23	833.6	11.9962
25	833.6	11.9962	24	833.6	11.9962

V= 1 TO 0 P- AND R-BRANCH TRANSITIONS FOR GADOLINIUM OXIDE

J OF P(J)	WAVE NO.	WAVELENGTH	J OF R(J)	WAVE NO.	WAVELENGTH
1	826.2	12.1036	0	826.2	12.1036
2	826.2	12.1036	1	826.2	12.1036
3	826.2	12.1036	2	826.2	12.1036
4	826.2	12.1036	3	826.2	12.1036
5	826.2	12.1036	4	826.2	12.1036
6	826.2	12.1036	5	826.2	12.1036
7	826.2	12.1036	6	826.2	12.1036
8	826.2	12.1036	7	826.2	12.1036
9	826.2	12.1036	8	826.2	12.1036
10	826.2	12.1036	9	826.2	12.1036
11	826.2	12.1036	10	826.2	12.1036
12	826.2	12.1036	11	826.2	12.1036
13	826.2	12.1036	12	826.2	12.1036
14	826.2	12.1036	13	826.2	12.1036
15	826.2	12.1036	14	826.2	12.1036
16	826.2	12.1036	15	826.2	12.1036
17	826.2	12.1036	16	826.2	12.1036
18	826.2	12.1036	17	826.2	12.1036
19	826.2	12.1036	18	826.2	12.1036
20	826.2	12.1036	19	826.2	12.1036
21	826.2	12.1036	20	826.2	12.1036
22	826.2	12.1036	21	826.2	12.1036
23	826.2	12.1036	22	826.2	12.1036
24	826.2	12.1036	23	826.2	12.1036
25	826.2	12.1036	24	826.2	12.1036

V= 2 TO 1 β- AND R-BRANCH TRANSITIONS FOR GADOLINIUM OXIDE

J OF P(J)	WAVE NO.	WAVELENGTH	J OF R(J)	WAVE NO.	WAVELENGTH
1	818.799	12.213	0	818.799	12.213
2	818.799	12.213	1	818.799	12.213
3	818.799	12.213	2	818.799	12.213
4	818.799	12.213	3	818.799	12.213
5	818.799	12.213	4	818.799	12.213
6	818.799	12.213	5	818.799	12.213
7	818.799	12.213	6	818.799	12.213
8	818.799	12.213	7	818.799	12.213
9	818.799	12.213	8	818.799	12.213
10	818.799	12.213	9	818.799	12.213
11	818.799	12.213	10	818.799	12.213
12	818.799	12.213	11	818.799	12.213
13	818.799	12.213	12	818.799	12.213
14	818.799	12.213	13	818.799	12.213
15	818.799	12.213	14	818.799	12.213
16	818.799	12.213	15	818.799	12.213
17	818.799	12.213	16	818.799	12.213
18	818.799	12.213	17	818.799	12.213
19	818.799	12.213	18	818.799	12.213
20	818.799	12.213	19	818.799	12.213
21	818.799	12.213	20	818.799	12.213
22	818.799	12.213	21	818.799	12.213
23	818.799	12.213	22	818.799	12.213
24	818.799	12.213	23	818.799	12.213
25	818.799	12.213	24	818.799	12.213

V= 3 TO 2 P- AND R-BRANCH TRANSITIONS FOR GADOLINIUM OXIDE

J OF P(J)	WAVE NO.	WAVELENGTH	J OF R(J)	WAVE NO.	WAVELENGTH
1	811.399	12.3244	0	811.399	12.3244
2	811.399	12.3244	1	811.399	12.3244
3	811.399	12.3244	2	811.399	12.3244
4	811.399	12.3244	3	811.399	12.3244
5	811.399	12.3244	4	811.399	12.3244
6	811.399	12.3244	5	811.399	12.3244
7	811.399	12.3244	6	811.399	12.3244
8	811.399	12.3244	7	811.399	12.3244
9	811.399	12.3244	8	811.399	12.3244
10	811.399	12.3244	9	811.399	12.3244
11	811.399	12.3244	10	811.399	12.3244
12	811.399	12.3244	11	811.399	12.3244
13	811.399	12.3244	12	811.399	12.3244
14	811.399	12.3244	13	811.399	12.3244
15	811.399	12.3244	14	811.399	12.3244
16	811.399	12.3244	15	811.399	12.3244
17	811.399	12.3244	16	811.399	12.3244
18	811.399	12.3244	17	811.399	12.3244
19	811.399	12.3244	18	811.399	12.3244
20	811.399	12.3244	19	811.399	12.3244
21	811.399	12.3244	20	811.399	12.3244
22	811.399	12.3244	21	811.399	12.3244
23	811.399	12.3244	22	811.399	12.3244
24	811.399	12.3244	23	811.399	12.3244
25	811.399	12.3244	24	811.399	12.3244

V= 4 TO 3 P- AND R-BRANCH TRANSITIONS FOR GADOLINIUM OXIDE

J OF P(J)	WAVE NO.	WAVELENGTH	J OF R(J)	WAVE NO.	WAVELENGTH
1	804.001	12.4378	0	804.001	12.4378
2	804.001	12.4378	1	804.001	12.4378
3	804.001	12.4378	2	804.001	12.4378
4	804.001	12.4378	3	804.001	12.4378
5	804.001	12.4378	4	804.001	12.4378
6	804.001	12.4378	5	804.001	12.4378
7	804.001	12.4378	6	804.001	12.4378
8	804.001	12.4378	7	804.001	12.4378
9	804.001	12.4378	8	804.001	12.4378
10	804.001	12.4378	9	804.001	12.4378
11	804.001	12.4378	10	804.001	12.4378
12	804.001	12.4378	11	804.001	12.4378
13	804.001	12.4378	12	804.001	12.4378
14	804.001	12.4378	13	804.001	12.4378
15	804.001	12.4378	14	804.001	12.4378
16	804.001	12.4378	15	804.001	12.4378
17	804.001	12.4378	16	804.001	12.4378
18	804.001	12.4378	17	804.001	12.4378
19	804.001	12.4378	18	804.001	12.4378
20	804.001	12.4378	19	804.001	12.4378
21	804.001	12.4378	20	804.001	12.4378
22	804.001	12.4378	21	804.001	12.4378
23	804.001	12.4378	22	804.001	12.4378
24	804.001	12.4378	23	804.001	12.4378
25	804.001	12.4378	24	804.001	12.4378

V= 5 TO 4 P- AND R-BRANCH TRANSITIONS FOR GADOLINIUM OXIDE

J OF P(J)	WAVE NO.	WAVELENGTH	J OF R(J)	WAVE NO.	WAVELENGTH
1	796.596	12.5534	0	796.596	12.5534
2	796.596	12.5534	1	796.596	12.5534
3	796.596	12.5534	2	796.596	12.5534
4	796.596	12.5534	3	796.596	12.5534
5	796.596	12.5534	4	796.596	12.5534
6	796.596	12.5534	5	796.596	12.5534
7	796.596	12.5534	6	796.596	12.5534
8	796.596	12.5534	7	796.596	12.5534
9	796.596	12.5534	8	796.596	12.5534
10	796.596	12.5534	9	796.596	12.5534
11	796.596	12.5534	10	796.596	12.5534
12	796.596	12.5534	11	796.596	12.5534
13	796.596	12.5534	12	796.596	12.5534
14	796.596	12.5534	13	796.596	12.5534
15	796.596	12.5534	14	796.596	12.5534
16	796.596	12.5534	15	796.596	12.5534
17	796.596	12.5534	16	796.596	12.5534
18	796.596	12.5534	17	796.596	12.5534
19	796.596	12.5534	18	796.596	12.5534
20	796.596	12.5534	19	796.596	12.5534
21	796.596	12.5534	20	796.596	12.5534
22	796.596	12.5534	21	796.596	12.5534
23	796.596	12.5534	22	796.596	12.5534
24	796.596	12.5534	23	796.596	12.5534
25	796.596	12.5534	24	796.596	12.5534

V= 6 TO 5 P- AND R-BRANCH TRANSITIONS FOR GADOLINIUM OXIDE

J OF P(J)	WAVE NO.	WAVELENGTH	J OF R(J)	WAVE NO.	WAVELENGTH
1	789.204	12.671	0	789.204	12.671
2	789.204	12.671	1	789.204	12.671
3	789.204	12.671	2	789.204	12.671
4	789.204	12.671	3	789.204	12.671
5	789.204	12.671	4	789.204	12.671
6	789.204	12.671	5	789.204	12.671
7	789.204	12.671	6	789.204	12.671
8	789.204	12.671	7	789.204	12.671
9	789.204	12.671	8	789.204	12.671
10	789.204	12.671	9	789.204	12.671
11	789.204	12.671	10	789.204	12.671
12	789.204	12.671	11	789.204	12.671
13	789.204	12.671	12	789.204	12.671
14	789.204	12.671	13	789.204	12.671
15	789.204	12.671	14	789.204	12.671
16	789.204	12.671	15	789.204	12.671
17	789.204	12.671	16	789.204	12.671
18	789.204	12.671	17	789.204	12.671
19	789.204	12.671	18	789.204	12.671
20	789.204	12.671	19	789.204	12.671
21	789.204	12.671	20	789.204	12.671
22	789.204	12.671	21	789.204	12.671
23	789.204	12.671	22	789.204	12.671
24	789.204	12.671	23	789.204	12.671
25	789.204	12.671	24	789.204	12.671

V= 7 TO 6 P- AND R-BRANCH TRANSITIONS FOR GADOLINIUM OXIDE

J OF P(J)	WAVE NO.	WAVELENGTH	J OF R(J)	WAVE NO.	WAVELENGTH
1	781.8	12.791	0	781.8	12.791
2	781.8	12.791	1	781.8	12.791
3	781.8	12.791	2	781.8	12.791
4	781.8	12.791	3	781.8	12.791
5	781.8	12.791	4	781.8	12.791
6	781.8	12.791	5	781.8	12.791
7	781.8	12.791	6	781.8	12.791
8	781.8	12.791	7	781.8	12.791
9	781.8	12.791	8	781.8	12.791
10	781.8	12.791	9	781.8	12.791
11	781.8	12.791	10	781.8	12.791
12	781.8	12.791	11	781.8	12.791
13	781.8	12.791	12	781.8	12.791
14	781.8	12.791	13	781.8	12.791
15	781.8	12.791	14	781.8	12.791
16	781.8	12.791	15	781.8	12.791
17	781.8	12.791	16	781.8	12.791
18	781.8	12.791	17	781.8	12.791
19	781.8	12.791	18	781.8	12.791
20	781.8	12.791	19	781.8	12.791
21	781.8	12.791	20	781.8	12.791
22	781.8	12.791	21	781.8	12.791
23	781.8	12.791	22	781.8	12.791
24	781.8	12.791	23	781.8	12.791
25	781.8	12.791	24	781.8	12.791

V= 8 TO 7 P- AND R-BRANCH TRANSITIONS FOR GADOLINIUM OXIDE

J OF P(J)	WAVE NO.	WAVELENGTH	J OF R(J)	WAVE NO.	WAVELENGTH
1	774.396	12.9133	0	774.396	12.9133
2	774.396	12.9133	1	774.396	12.9133
3	774.396	12.9133	2	774.396	12.9133
4	774.396	12.9133	3	774.396	12.9133
5	774.396	12.9133	4	774.396	12.9133
6	774.396	12.9133	5	774.396	12.9133
7	774.396	12.9133	6	774.396	12.9133
8	774.396	12.9133	7	774.396	12.9133
9	774.396	12.9133	8	774.396	12.9133
10	774.396	12.9133	9	774.396	12.9133
11	774.396	12.9133	10	774.396	12.9133
12	774.396	12.9133	11	774.396	12.9133
13	774.396	12.9133	12	774.396	12.9133
14	774.396	12.9133	13	774.396	12.9133
15	774.396	12.9133	14	774.396	12.9133
16	774.396	12.9133	15	774.396	12.9133
17	774.396	12.9133	16	774.396	12.9133
18	774.396	12.9133	17	774.396	12.9133
19	774.396	12.9133	18	774.396	12.9133
20	774.396	12.9133	19	774.396	12.9133
21	774.396	12.9133	20	774.396	12.9133
22	774.396	12.9133	21	774.396	12.9133
23	774.396	12.9133	22	774.396	12.9133
24	774.396	12.9133	23	774.396	12.9133
25	774.396	12.9133	24	774.396	12.9133

V= 9 TO 8 P- AND R-BRANCH TRANSITIONS FOR GADOLINIUM OXIDE

J OF P(J)	WAVE NO.	WAVELENGTH	J OF R(J)	WAVE NO.	WAVELENGTH
1	766.998	13.0378	0	766.998	13.0378
2	766.998	13.0378	1	766.998	13.0378
3	766.998	13.0378	2	766.998	13.0378
4	766.998	13.0378	3	766.998	13.0378
5	766.998	13.0378	4	766.998	13.0378
6	766.998	13.0378	5	766.998	13.0378
7	766.998	13.0378	6	766.998	13.0378
8	766.998	13.0378	7	766.998	13.0378
9	766.998	13.0378	8	766.998	13.0378
10	766.998	13.0378	9	766.998	13.0378
11	766.998	13.0378	10	766.998	13.0378
12	766.998	13.0378	11	766.998	13.0378
13	766.998	13.0378	12	766.998	13.0378
14	766.998	13.0378	13	766.998	13.0378
15	766.998	13.0378	14	766.998	13.0378
16	766.998	13.0378	15	766.998	13.0378
17	766.998	13.0378	16	766.998	13.0378
18	766.998	13.0378	17	766.998	13.0378
19	766.998	13.0378	18	766.998	13.0378
20	766.998	13.0378	19	766.998	13.0378
21	766.998	13.0378	20	766.998	13.0378
22	766.998	13.0378	21	766.998	13.0378
23	766.998	13.0378	22	766.998	13.0378
24	766.998	13.0378	23	766.998	13.0378
25	766.998	13.0378	24	766.998	13.0378

V= 10 TO 9 P- AND R-BRANCH TRANSITIONS FOR GADOLINIUM OXIDE

```
REM DIATOMIC MOLECULAR SPECTRA
READ A,B
READ C,D
DIM Y(10,10)
FOR M=0 TO D
FOR L=0 TO C
READ Y(L+1,M+1)
NEXT L
NEXT M
FOR V=1 TO A
PRINT 'V=',V,'TO', V-1,'P- AND R-BRANCH TRANSITIONS FOR',
PRINT'LANTHANUM OXIDE'
PRINT 'J OF P(J)','WAVE NO.','WAVELENGTH','J OF R(J)',
PRINT 'WAVE NO.','WAVELENGTH'
FOR J=1 TO B
LET I=J-1
LET S1=0
LET S2=0
LET G=0
FOR L=0 TO C
LET G=G+Y(L+1,1)*((V+.5)**L-(V-.5)**L)
NEXT L
FOR L=0 TO C
FOR M=1 TO D
LET R=Y(L+1,M+1)
LET E=(V+.5)**L*(I+1)**M*(I+2)**M
LET S1=S1+R*((V+.5)**L*J**M*(J-1)**M-(V-.5)**L*J**M*(J+1)**M)
LET F=(V-.5)**L*I**M*(I+1)**M
LET S2=S2+R*(E-F)
NEXT M
NEXT L
LET       S1=S1+G
LET S2=S2+G
PRINT J,S1,10000/S1,I,S2,10000/S2
NEXT J
PRINT
PRINT
PRINT
PRINT
NEXT V
DATA 10,25
DATA 4,1
DATA 0.0,817.26,-3.097,.0406,0.0
DATA 0.0,0.0,0.0,0.0,0.0
END
```

J OF P(J)	WAVE NO.	WAVELENGTH	J OF R(J)	WAVE NO.	WAVELENGTH
1	811.198	12.3275	0	811.198	12.3275
2	811.198	12.3275	1	811.198	12.3275
3	811.198	12.3275	2	811.198	12.3275
4	811.198	12.3275	3	811.198	12.3275
5	811.198	12.3275	4	811.198	12.3275
6	811.198	12.3275	5	811.198	12.3275
7	811.198	12.3275	6	811.198	12.3275
8	811.198	12.3275	7	811.198	12.3275
9	811.198	12.3275	8	811.198	12.3275
10	811.198	12.3275	9	811.198	12.3275
11	811.198	12.3275	10	811.198	12.3275
12	811.198	12.3275	11	811.198	12.3275
13	811.198	12.3275	12	811.198	12.3275
14	811.198	12.3275	13	811.198	12.3275
15	811.198	12.3275	14	811.198	12.3275
16	811.198	12.3275	15	811.198	12.3275
17	811.198	12.3275	16	811.198	12.3275
18	811.198	12.3275	17	811.198	12.3275
19	811.198	12.3275	18	811.198	12.3275
20	811.198	12.3275	19	811.198	12.3275
21	811.198	12.3275	20	811.198	12.3275
22	811.198	12.3275	21	811.198	12.3275
23	811.198	12.3275	22	811.198	12.3275
24	811.198	12.3275	23	811.198	12.3275
25	811.198	12.3275	24	811.198	12.3275

V= 1 TO 0 P- AND R-BRANCH TRANSITIONS FOR LANTHANUM OXIDE

J OF P(J)	WAVE NO.	WAVELENGTH	J OF R(J)	WAVE NO.	WAVELENGTH
1	805.369	12.4167	0	805.369	12.4167
2	805.369	12.4167	1	805.369	12.4167
3	805.369	12.4167	2	805.369	12.4167
4	805.369	12.4167	3	805.369	12.4167
5	805.369	12.4167	4	805.369	12.4167
6	805.369	12.4167	5	805.369	12.4167
7	805.369	12.4167	6	805.369	12.4167
8	805.369	12.4167	7	805.369	12.4167
9	805.369	12.4167	8	805.369	12.4167
10	805.369	12.4167	9	805.369	12.4167
11	805.369	12.4167	10	805.369	12.4167
12	805.369	12.4167	11	805.369	12.4167
13	805.369	12.4167	12	805.369	12.4167
14	805.369	12.4167	13	805.369	12.4167
15	805.369	12.4167	14	805.369	12.4167
16	805.369	12.4167	15	805.369	12.4167
17	805.369	12.4167	16	805.369	12.4167
18	805.369	12.4167	17	805.369	12.4167
19	805.369	12.4167	18	805.369	12.4167
20	805.369	12.4167	19	805.369	12.4167
21	805.369	12.4167	20	805.369	12.4167
22	805.369	12.4167	21	805.369	12.4167
23	805.369	12.4167	22	805.369	12.4167
24	805.369	12.4167	23	805.369	12.4167
25	805.369	12.4167	24	805.369	12.4167

V= 2 TO 1 P- AND R-BRANCH TRANSITIONS FOR LANTHANUM OXIDE

J OF P(J)	WAVE NO.	WAVELENGTH	J OF R(J)	WAVE NO.	WAVELENGTH
1	799.783	12.5034	0	799.783	12.5034
2	799.783	12.5034	1	799.783	12.5034
3	799.783	12.5034	2	799.783	12.5034
4	799.783	12.5034	3	799.783	12.5034
5	799.783	12.5034	4	799.783	12.5034
6	799.783	12.5034	5	799.783	12.5034
7	799.783	12.5034	6	799.783	12.5034
8	799.783	12.5034	7	799.783	12.5034
9	799.783	12.5034	8	799.783	12.5034
10	799.783	12.5034	9	799.783	12.5034
11	799.783	12.5034	10	799.783	12.5034
12	799.783	12.5034	11	799.783	12.5034
13	799.783	12.5034	12	799.783	12.5034
14	799.783	12.5034	13	799.783	12.5034
15	799.783	12.5034	14	799.783	12.5034
16	799.783	12.5034	15	799.783	12.5034
17	799.783	12.5034	16	799.783	12.5034
18	799.783	12.5034	17	799.783	12.5034
19	799.783	12.5034	18	799.783	12.5034
20	799.783	12.5034	19	799.783	12.5034
21	799.783	12.5034	20	799.783	12.5034
22	799.783	12.5034	21	799.783	12.5034
23	799.783	12.5034	22	799.783	12.5034
24	799.783	12.5034	23	799.783	12.5034
25	799.783	12.5034	24	799.783	12.5034

V= 3 TO 2 P- AND R-BRANCH TRANSITIONS FOR LANTHANUM OXIDE

J OF P(J)	WAVE NO.	WAVELENGTH	J OF R(J)	WAVE NO.	WAVELENGTH
1	794.441	12.5875	0	794.441	12.5875
2	794.441	12.5875	1	794.441	12.5875
3	794.441	12.5875	2	794.441	12.5875
4	794.441	12.5875	3	794.441	12.5875
5	794.441	12.5875	4	794.441	12.5875
6	794.441	12.5875	5	794.441	12.5875
7	794.441	12.5875	6	794.441	12.5875
8	794.441	12.5875	7	794.441	12.5875
9	794.441	12.5875	8	794.441	12.5875
10	794.441	12.5875	9	794.441	12.5875
11	794.441	12.5875	10	794.441	12.5875
12	794.441	12.5875	11	794.441	12.5875
13	794.441	12.5875	12	794.441	12.5875
14	794.441	12.5875	13	794.441	12.5875
15	794.441	12.5875	14	794.441	12.5875
16	794.441	12.5875	15	794.441	12.5875
17	794.441	12.5875	16	794.441	12.5875
18	794.441	12.5875	17	794.441	12.5875
19	794.441	12.5875	18	794.441	12.5875
20	794.441	12.5875	19	794.441	12.5875
21	794.441	12.5875	20	794.441	12.5875
22	794.441	12.5875	21	794.441	12.5875
23	794.441	12.5875	22	794.441	12.5875
24	794.441	12.5875	23	794.441	12.5875
25	794.441	12.5875	24	794.441	12.5875

V= 4 TO3 P- ANDR-BRANCH TRANSITIONS FOR LANTHANUM OXIDE

J OF P(J)	WAVE NO.	WAVELENGTH	J OF R(J)	WAVE NO.	WAVELENGTH
1	789.346	12.6687	0	789.346	12.6687
2	789.346	12.6687	1	789.346	12.6687
3	789.346	12.6687	2	789.346	12.6687
4	789.346	12.6687	3	789.346	12.6687
5	789.346	12.6687	4	789.346	12.6687
6	789.346	12.6687	5	789.346	12.6687
7	789.346	12.6687	6	789.346	12.6687
8	789.346	12.6687	7	789.346	12.6687
9	789.346	12.6687	8	789.346	12.6687
10	789.346	12.6687	9	789.346	12.6687
11	789.346	12.6687	10	789.346	12.6687
12	789.346	12.6687	11	789.346	12.6687
13	789.346	12.6687	12	789.346	12.6687
14	789.346	12.6687	13	789.346	12.6687
15	789.346	12.6687	14	789.346	12.6687
16	789.346	12.6687	15	789.346	12.6687
17	789.346	12.6687	16	789.346	12.6687
18	789.346	12.6687	17	789.346	12.6687
19	789.346	12.6687	18	789.346	12.6687
20	789.346	12.6687	19	789.346	12.6687
21	789.346	12.6687	20	789.346	12.6687
22	789.346	12.6687	21	789.346	12.6687
23	789.346	12.6687	22	789.346	12.6687
24	789.346	12.6687	23	789.346	12.6687
25	789.346	12.6687	24	789.346	12.6687

V= 5 TO 4 P- AND R-BRANCH TRANSITIONS FOR LANTHANUM OXIDE

J OF P(J)	WAVE NO.	WAVELENGTH	J OF R(J)	WAVE NO.	WAVELENGTH
1	784.487	12.7472	0	784.487	12.7472
2	784.487	12.7472	1	784.487	12.7472
3	784.487	12.7472	2	784.487	12.7472
4	784.487	12.7472	3	784.487	12.7472
5	784.487	12.7472	4	784.487	12.7472
6	784.487	12.7472	5	784.487	12.7472
7	784.487	12.7472	6	784.487	12.7472
8	784.487	12.7472	7	784.487	12.7472
9	784.487	12.7472	8	784.487	12.7472
10	784.487	12.7472	9	784.487	12.7472
11	784.487	12.7472	10	784.487	12.7472
12	784.487	12.7472	11	784.487	12.7472
13	784.487	12.7472	12	784.487	12.7472
14	784.487	12.7472	13	784.487	12.7472
15	784.487	12.7472	14	784.487	12.7472
16	784.487	12.7472	15	784.487	12.7472
17	784.487	12.7472	16	784.487	12.7472
18	784.487	12.7472	17	784.487	12.7472
19	784.487	12.7472	18	784.487	12.7472
20	784.487	12.7472	19	784.487	12.7472
21	784.487	12.7472	20	784.487	12.7472
22	784.487	12.7472	21	784.487	12.7472
23	784.487	12.7472	22	784.487	12.7472
24	784.487	12.7472	23	784.487	12.7472
25	784.487	12.7472	24	784.487	12.7472

V= 6 TO 5 P- AND R-BRANCH TRANSITIONS FOR LANTHANUM OXIDE

J OF P(J)	WAVE NO.	WAVELENGTH	J OF R(J)	WAVE NO.	WAVELENGTH
1	779.883	12.8224	0	779.883	12.8224
2	779.883	12.8224	1	779.883	12.8224
3	779.883	12.8224	2	779.883	12.8224
4	779.883	12.8224	3	779.883	12.8224
5	779.883	12.8224	4	779.883	12.8224
6	779.883	12.8224	5	779.883	12.8224
7	779.883	12.8224	6	779.883	12.8224
8	779.883	12.8224	7	779.883	12.8224
9	779.883	12.8224	8	779.883	12.8224
10	779.883	12.8224	9	779.883	12.8224
11	779.883	12.8224	10	779.883	12.8224
12	779.883	12.8224	11	779.883	12.8224
13	779.883	12.8224	12	779.883	12.8224
14	779.883	12.8224	13	779.883	12.8224
15	779.883	12.8224	14	779.883	12.8224
16	779.883	12.8224	15	779.883	12.8224
17	779.883	12.8224	16	779.883	12.8224
18	779.883	12.8224	17	779.883	12.8224
19	779.883	12.8224	18	779.883	12.8224
20	779.883	12.8224	19	779.883	12.8224
21	779.883	12.8224	20	779.883	12.8224
22	779.883	12.8224	21	779.883	12.8224
23	779.883	12.8224	22	779.883	12.8224
24	779.883	12.8224	23	779.883	12.8224
25	779.883	12.8224	24	779.883	12.8224

V= 7 TO 6 P- AND R-BRANCH TRANSITIONS FOR LANTHANUM OXIDE

J OF P(J)	WAVE NO.	WAVELENGTH	J OF R(J)	WAVE NO.	WAVELENGTH
1	775.513	12.8947	0	775.513	12.8947
2	775.513	12.8947	1	775.513	12.8947
3	775.513	12.8947	2	775.513	12.8947
4	775.513	12.8947	3	775.513	12.8947
5	775.513	12.8947	4	775.513	12.8947
6	775.513	12.8947	5	775.513	12.8947
7	775.513	12.8947	6	775.513	12.8947
8	775.513	12.8947	7	775.513	12.8947
9	775.513	12.8947	8	775.513	12.8947
10	775.513	12.8947	9	775.513	12.8947
11	775.513	12.8947	10	775.513	12.8947
12	775.513	12.8947	11	775.513	12.8947
13	775.513	12.8947	12	775.513	12.8947
14	775.513	12.8947	13	775.513	12.8947
15	775.513	12.8947	14	775.513	12.8947
16	775.513	12.8947	15	775.513	12.8947
17	775.513	12.8947	16	775.513	12.8947
18	775.513	12.8947	17	775.513	12.8947
19	775.513	12.8947	18	775.513	12.8947
20	775.513	12.8947	19	775.513	12.8947
21	775.513	12.8947	20	775.513	12.8947
22	775.513	12.8947	21	775.513	12.8947
23	775.513	12.8947	22	775.513	12.8947
24	775.513	12.8947	23	775.513	12.8947
25	775.513	12.8947	24	775.513	12.8947

V= 8 TO 7 P- AND R-BRANCH TRANSITIONS FOR LANTHANUM OXIDE

J OF P(J)	WAVE NO.	WAVELENGTH	J OF R(J)	WAVE NO.	WAVELENGTH
1	771.386	12.9637	0	771.386	12.9637
2	771.386	12.9637	1	771.386	12.9637
3	771.386	12.9637	2	771.386	12.9637
4	771.386	12.9637	3	771.386	12.9637
5	771.386	12.9637	4	771.386	12.9637
6	771.386	12.9637	5	771.386	12.9637
7	771.386	12.9637	6	771.386	12.9637
8	771.386	12.9637	7	771.386	12.9637
9	771.386	12.9637	8	771.386	12.9637
10	771.386	12.9637	9	771.386	12.9637
11	771.386	12.9637	10	771.386	12.9637
12	771.386	12.9637	11	771.386	12.9637
13	771.386	12.9637	12	771.386	12.9637
14	771.386	12.9637	13	771.386	12.9637
15	771.386	12.9637	14	771.386	12.9637
16	771.386	12.9637	15	771.386	12.9637
17	771.386	12.9637	16	771.386	12.9637
18	771.386	12.9637	17	771.386	12.9637
19	771.386	12.9637	18	771.386	12.9637
20	771.386	12.9637	19	771.386	12.9637
21	771.386	12.9637	20	771.386	12.9637
22	771.386	12.9637	21	771.386	12.9637
23	771.386	12.9637	22	771.386	12.9637
24	771.386	12.9637	23	771.386	12.9637
25	771.386	12.9637	24	771.386	12.9637

V= 9 TO 8 P- AND R-BRANCH TRANSITIONS FOR LANTHANUM OXIDE

J OF P(J)	WAVE NO.	WAVELENGTH	J OF R(J)	WAVE NO.	WAVELENGTH
1	767.508	13.0292	0	767.508	13.0292
2	767.508	13.0292	1	767.508	13.0292
3	767.508	13.0292	2	767.508	13.0292
4	767.508	13.0292	3	767.508	13.0292
5	767.508	13.0292	4	767.508	13.0292
6	767.508	13.0292	5	767.508	13.0292
7	767.508	13.0292	6	767.508	13.0292
8	767.508	13.0292	7	767.508	13.0292
9	767.508	13.0292	8	767.508	13.0292
10	767.508	13.0292	9	767.508	13.0292
11	767.508	13.0292	10	767.508	13.0292
12	767.508	13.0292	11	767.508	13.0292
13	767.508	13.0292	12	767.508	13.0292
14	767.508	13.0292	13	767.508	13.0292
15	767.508	13.0292	14	767.508	13.0292
16	767.508	13.0292	15	767.508	13.0292
17	767.508	13.0292	16	767.508	13.0292
18	767.508	13.0292	17	767.508	13.0292
19	767.508	13.0292	18	767.508	13.0292
20	767.508	13.0292	19	767.508	13.0292
21	767.508	13.0292	20	767.508	13.0292
22	767.508	13.0292	21	767.508	13.0292
23	767.508	13.0292	22	767.508	13.0292
24	767.508	13.0292	23	767.508	13.0292
25	767.508	13.0292	24	767.508	13.0292

V= 10 TO 9 P- AND R-BRANCH TRANSITIONS FOR LANTHANUM OXIDE

```
REM DIATOMIC MOLECULAR SPECTRA
READ A,B
READ C,D
DIM Y(10,10)
FOR M=0 TO D
FOR L=0 TO C
READ Y(L+1,M+1)
NEXT L
NEXT M
FOR V=1 TO A
PRINT 'V=',V,'TO', V-1,'P- AND R-BRANCH TRANSITIONS FOR',
PRINT'PRASODYMIUM OXIDE'
PRINT 'J OF P(J)','WAVE NO.','WAVELENGTH','J OF R(J)',
PRINT 'WAVE NO.','WAVELENGTH'
FOR J=1 TO B
LET I=J-1
LET S1=0
LET S2=0
LET G=0
FOR L=0 TO C
LET G=G+Y(L+1,1)*((V+.5)**L-(V-.5)**L)
NEXT L
FOR L=0 TO C
FOR M=1 TO D
LET R=Y(L+1,M+1)
LET E=(V+.5)**L*(I+1)**M*(I+2)**M
LET S1=S1+R*((V+.5)**L*J**M*(J-1)**M-(V-.5)**L*J**M*(J+1)**M)
LET F=(V-.5)**L*I**M*(I+1)**M
LET S2=S2+R*(E-F)
NEXT M
NEXT L
LET       S1=S1+G
LET S2=S2+G
PRINT J,S1,10000/S1,I,S2,10000/S2
NEXT J
PRINT
PRINT
PRINT
PRINT
NEXT V
DATA 10,25
DATA 3,1
DATA 0.0,818.9,-1.2,0.0
DATA 0.0,0.0,0.0,0.0
END
```

J OF P(J)	WAVE NO.	WAVELENGTH	J OF R(J)	WAVE NO.	WAVELENGTH
1	816.5	12.2474	0	816.5	12.2474
2	816.5	12.2474	1	816.5	12.2474
3	816.5	12.2474	2	816.5	12.2474
4	816.5	12.2474	3	816.5	12.2474
5	816.5	12.2474	4	816.5	12.2474
6	816.5	12.2474	5	816.5	12.2474
7	816.5	12.2474	6	816.5	12.2474
8	816.5	12.2474	7	816.5	12.2474
9	816.5	12.2474	8	816.5	12.2474
10	816.5	12.2474	9	816.5	12.2474
11	816.5	12.2474	10	816.5	12.2474
12	816.5	12.2474	11	816.5	12.2474
13	816.5	12.2474	12	816.5	12.2474
14	816.5	12.2474	13	816.5	12.2474
15	816.5	12.2474	14	816.5	12.2474
16	816.5	12.2474	15	816.5	12.2474
17	816.5	12.2474	16	816.5	12.2474
18	816.5	12.2474	17	816.5	12.2474
19	816.5	12.2474	18	816.5	12.2474
20	816.5	12.2474	19	816.5	12.2474
21	816.5	12.2474	20	816.5	12.2474
22	816.5	12.2474	21	816.5	12.2474
23	816.5	12.2474	22	816.5	12.2474
24	816.5	12.2474	23	816.5	12.2474
25	816.5	12.2474	24	816.5	12.2474

V= 1 TO 0 P- AND R-BRANCH TRANSITIONS FOR PRASEODYMIUM OXIDE

J OF P(J)	WAVE NO.	WAVELENGTH	J OF R(J)	WAVE NO.	WAVELENGTH
1	814.1	12.2835	0	814.1	12.2835
2	814.1	12.2835	1	814.1	12.2835
3	814.1	12.2835	2	814.1	12.2835
4	814.1	12.2835	3	814.1	12.2835
5	814.1	12.2835	4	814.1	12.2835
6	814.1	12.2835	5	814.1	12.2835
7	814.1	12.2835	6	814.1	12.2835
8	814.1	12.2835	7	814.1	12.2835
9	814.1	12.2835	8	814.1	12.2835
10	814.1	12.2835	9	814.1	12.2835
11	814.1	12.2835	10	814.1	12.2835
12	814.1	12.2835	11	814.1	12.2835
13	814.1	12.2835	12	814.1	12.2835
14	814.1	12.2835	13	814.1	12.2835
15	814.1	12.2835	14	814.1	12.2835
16	814.1	12.2835	15	814.1	12.2835
17	814.1	12.2835	16	814.1	12.2835
18	814.1	12.2835	17	814.1	12.2835
19	814.1	12.2835	18	814.1	12.2835
20	814.1	12.2835	19	814.1	12.2835
21	814.1	12.2835	20	814.1	12.2835
22	814.1	12.2835	21	814.1	12.2835
23	814.1	12.2835	22	814.1	12.2835
24	814.1	12.2835	23	814.1	12.2835
25	814.1	12.2835	24	814.1	12.2835

V= 2 TO 1 P- AND R-BRANCH TRANSITIONS FOR PRASEODYMIUM OXIDE

J OF P(J)	WAVE NO.	WAVELENGTH	J OF R(J)	WAVE NO.	WAVELENGTH
1	811.699	12.3198	0	811.699	12.3198
2	811.699	12.3198	1	811.699	12.3198
3	811.699	12.3198	2	811.699	12.3198
4	811.699	12.3198	3	811.699	12.3198
5	811.699	12.3198	4	811.699	12.3198
6	811.699	12.3198	5	811.699	12.3198
7	811.699	12.3198	6	811.699	12.3198
8	811.699	12.3198	7	811.699	12.3198
9	811.699	12.3198	8	811.699	12.3198
10	811.699	12.3198	9	811.699	12.3198
11	811.699	12.3198	10	811.699	12.3198
12	811.699	12.3198	11	811.699	12.3198
13	811.699	12.3198	12	811.699	12.3198
14	811.699	12.3198	13	811.699	12.3198
15	811.699	12.3198	14	811.699	12.3198
16	811.699	12.3198	15	811.699	12.3198
17	811.699	12.3198	16	811.699	12.3198
18	811.699	12.3198	17	811.699	12.3198
19	811.699	12.3198	18	811.699	12.3198
20	811.699	12.3198	19	811.699	12.3198
21	811.699	12.3198	20	811.699	12.3198
22	811.699	12.3198	21	811.699	12.3198
23	811.699	12.3198	22	811.699	12.3198
24	811.699	12.3198	23	811.699	12.3198
25	811.699	12.3198	24	811.699	12.3198

V= 3 TO 2 P- AND R-BRANCH TRANSITIONS FOR PRASEODYMIUM OXIDE

J OF P(J)	WAVE NO.	WAVELENGTH	J OF R(J)	WAVE NO.	WAVELENGTH
1	809.299	12.3564	0	809.299	12.3564
2	809.299	12.3564	1	809.299	12.3564
3	809.299	12.3564	2	809.299	12.3564
4	809.299	12.3564	3	809.299	12.3564
5	809.299	12.3564	4	809.299	12.3564
6	809.299	12.3564	5	809.299	12.3564
7	809.299	12.3564	6	809.299	12.3564
8	809.299	12.3564	7	809.299	12.3564
9	809.299	12.3564	8	809.299	12.3564
10	809.299	12.3564	9	809.299	12.3564
11	809.299	12.3564	10	809.299	12.3564
12	809.299	12.3564	11	809.299	12.3564
13	809.299	12.3564	12	809.299	12.3564
14	809.299	12.3564	13	809.299	12.3564
15	809.299	12.3564	14	809.299	12.3564
16	809.299	12.3564	15	809.299	12.3564
17	809.299	12.3564	16	809.299	12.3564
18	809.299	12.3564	17	809.299	12.3564
19	809.299	12.3564	18	809.299	12.3564
20	809.299	12.3564	19	809.299	12.3564
21	809.299	12.3564	20	809.299	12.3564
22	809.299	12.3564	21	809.299	12.3564
23	809.299	12.3564	22	809.299	12.3564
24	809.299	12.3564	23	809.299	12.3564
25	809.299	12.3564	24	809.299	12.3564

V= 4 TO 3 P- AND R-BRANCH TRANSITIONS FOR PRASEODYMIUM OXIDE

J OF P(J)	WAVE NO.	WAVELENGTH	J OF R(J)	WAVE NO.	WAVELENGTH
1	806.901	12.3931	0	806.901	12.3931
2	806.901	12.3931	1	806.901	12.3931
3	806.901	12.3931	2	806.901	12.3931
4	806.901	12.3931	3	806.901	12.3931
5	806.901	12.3931	4	806.901	12.3931
6	806.901	12.3931	5	806.901	12.3931
7	806.901	12.3931	6	806.901	12.3931
8	806.901	12.3931	7	806.901	12.3931
9	806.901	12.3931	8	806.901	12.3931
10	806.901	12.3931	9	806.901	12.3931
11	806.901	12.3931	10	806.901	12.3931
12	806.901	12.3931	11	806.901	12.3931
13	806.901	12.3931	12	806.901	12.3931
14	806.901	12.3931	13	806.901	12.3931
15	806.901	12.3931	14	806.901	12.3931
16	806.901	12.3931	15	806.901	12.3931
17	806.901	12.3931	16	806.901	12.3931
18	806.901	12.3931	17	806.901	12.3931
19	806.901	12.3931	18	806.901	12.3931
20	806.901	12.3931	19	806.901	12.3931
21	806.901	12.3931	20	806.901	12.3931
22	806.901	12.3931	21	806.901	12.3931
23	806.901	12.3931	22	806.901	12.3931
24	806.901	12.3931	23	806.901	12.3931
25	806.901	12.3931	24	806.901	12.3931

V= 5 TO 4 P- AND R-BRANCH TRANSITIONS FOR PRASEODYMIUM OXIDE

J OF P(J)	WAVE NO.	WAVELENGTH	J OF R(J)	WAVE NO.	WAVELENGTH
1	804.496	12.4301	0	804.496	12.4301
2	804.496	12.4301	1	804.496	12.4301
3	804.496	12.4301	2	804.496	12.4301
4	804.496	12.4301	3	804.496	12.4301
5	804.496	12.4301	4	804.496	12.4301
6	804.496	12.4301	5	804.496	12.4301
7	804.496	12.4301	6	804.496	12.4301
8	804.496	12.4301	7	804.496	12.4301
9	804.496	12.4301	8	804.496	12.4301
10	804.496	12.4301	9	804.496	12.4301
11	804.496	12.4301	10	804.496	12.4301
12	804.496	12.4301	11	804.496	12.4301
13	804.496	12.4301	12	804.496	12.4301
14	804.496	12.4301	13	804.496	12.4301
15	804.496	12.4301	14	804.496	12.4301
16	804.496	12.4301	15	804.496	12.4301
17	804.496	12.4301	16	804.496	12.4301
18	804.496	12.4301	17	804.496	12.4301
19	804.496	12.4301	18	804.496	12.4301
20	804.496	12.4301	19	804.496	12.4301
21	804.496	12.4301	20	804.496	12.4301
22	804.496	12.4301	21	804.496	12.4301
23	804.496	12.4301	22	804.496	12.4301
24	804.496	12.4301	23	804.496	12.4301
25	804.496	12.4301	24	804.496	12.4301

V= 6 TO 5 P- AND R-BRANCH TRANSITIONS FOR PRASEODYMIUM OXIDE

J OF P(J)	WAVE NO.	WAVELENGTH	J OF R(J)	WAVE NO.	WAVELENGTH
1	802.103	12.4672	0	802.103	12.4672
2	802.103	12.4672	1	802.103	12.4672
3	802.103	12.4672	2	802.103	12.4672
4	802.103	12.4672	3	802.103	12.4672
5	802.103	12.4672	4	802.103	12.4672
6	802.103	12.4672	5	802.103	12.4672
7	802.103	12.4672	6	802.103	12.4672
8	802.103	12.4672	7	802.103	12.4672
9	802.103	12.4672	8	802.103	12.4672
10	802.103	12.4672	9	802.103	12.4672
11	802.103	12.4672	10	802.103	12.4672
12	802.103	12.4672	11	802.103	12.4672
13	802.103	12.4672	12	802.103	12.4672
14	802.103	12.4672	13	802.103	12.4672
15	802.103	12.4672	14	802.103	12.4672
16	802.103	12.4672	15	802.103	12.4672
17	802.103	12.4672	16	802.103	12.4672
18	802.103	12.4672	17	802.103	12.4672
19	802.103	12.4672	18	802.103	12.4672
20	802.103	12.4672	19	802.103	12.4672
21	802.103	12.4672	20	802.103	12.4672
22	802.103	12.4672	21	802.103	12.4672
23	802.103	12.4672	22	802.103	12.4672
24	802.103	12.4672	23	802.103	12.4672
25	802.103	12.4672	24	802.103	12.4672

V= 7 TO 6 P- AND R-BRANCH TRANSITIONS FOR PRASEODYMIUM OXIDE

J OF P(J)	WAVE NO.	WAVELENGTH	J OF R(J)	WAVE NO.	WAVELENGTH
1	799.7	12.5047	0	799.7	12.5047
2	799.7	12.5047	1	799.7	12.5047
3	799.7	12.5047	2	799.7	12.5047
4	799.7	12.5047	3	799.7	12.5047
5	799.7	12.5047	4	799.7	12.5047
6	799.7	12.5047	5	799.7	12.5047
7	799.7	12.5047	6	799.7	12.5047
8	799.7	12.5047	7	799.7	12.5047
9	799.7	12.5047	8	799.7	12.5047
10	799.7	12.5047	9	799.7	12.5047
11	799.7	12.5047	10	799.7	12.5047
12	799.7	12.5047	11	799.7	12.5047
13	799.7	12.5047	12	799.7	12.5047
14	799.7	12.5047	13	799.7	12.5047
15	799.7	12.5047	14	799.7	12.5047
16	799.7	12.5047	15	799.7	12.5047
17	799.7	12.5047	16	799.7	12.5047
18	799.7	12.5047	17	799.7	12.5047
19	799.7	12.5047	18	799.7	12.5047
20	799.7	12.5047	19	799.7	12.5047
21	799.7	12.5047	20	799.7	12.5047
22	799.7	12.5047	21	799.7	12.5047
23	799.7	12.5047	22	799.7	12.5047
24	799.7	12.5047	23	799.7	12.5047
25	799.7	12.5047	24	799.7	12.5047

V= 8 TO 7 P- AND R-BRANCH TRANSITIONS FOR PRASEODYMIUM OXIDE

J OF P(J)	WAVE NO.	WAVELENGTH	J OF R(J)	WAVE NO.	WAVELENGTH
1	797.296	12.5424	0	797.296	12.5424
2	797.296	12.5424	1	797.296	12.5424
3	797.296	12.5424	2	797.296	12.5424
4	797.296	12.5424	3	797.296	12.5424
5	797.296	12.5424	4	797.296	12.5424
6	797.296	12.5424	5	797.296	12.5424
7	797.296	12.5424	6	797.296	12.5424
8	797.296	12.5424	7	797.296	12.5424
9	797.296	12.5424	8	797.296	12.5424
10	797.296	12.5424	9	797.296	12.5424
11	797.296	12.5424	10	797.296	12.5424
12	797.296	12.5424	11	797.296	12.5424
13	797.296	12.5424	12	797.296	12.5424
14	797.296	12.5424	13	797.296	12.5424
15	797.296	12.5424	14	797.296	12.5424
16	797.296	12.5424	15	797.296	12.5424
17	797.296	12.5424	16	797.296	12.5424
18	797.296	12.5424	17	797.296	12.5424
19	797.296	12.5424	18	797.296	12.5424
20	797.296	12.5424	19	797.296	12.5424
21	797.296	12.5424	20	797.296	12.5424
22	797.296	12.5424	21	797.296	12.5424
23	797.296	12.5424	22	797.296	12.5424
24	797.296	12.5424	23	797.296	12.5424
25	797.296	12.5424	24	797.296	12.5424

V= 9 TO 8 P- AND R-BRANCH TRANSITIONS FOR PRASEODYMIUM OXIDE

J OF P(J)	WAVE NO.	WAVELENGTH	J OF R(J)	WAVE NO.	WAVELENGTH
1	794.898	12.5802	0	794.898	12.5802
2	794.898	12.5802	1	794.898	12.5802
3	794.898	12.5802	2	794.898	12.5802
4	794.898	12.5802	3	794.898	12.5802
5	794.898	12.5802	4	794.898	12.5802
6	794.898	12.5802	5	794.898	12.5802
7	794.898	12.5802	6	794.898	12.5802
8	794.898	12.5802	7	794.898	12.5802
9	794.898	12.5802	8	794.898	12.5802
10	794.898	12.5802	9	794.898	12.5802
11	794.898	12.5802	10	794.898	12.5802
12	794.898	12.5802	11	794.898	12.5802
13	794.898	12.5802	12	794.898	12.5802
14	794.898	12.5802	13	794.898	12.5802
15	794.898	12.5802	14	794.898	12.5802
16	794.898	12.5802	15	794.898	12.5802
17	794.898	12.5802	16	794.898	12.5802
18	794.898	12.5802	17	794.898	12.5802
19	794.898	12.5802	18	794.898	12.5802
20	794.898	12.5802	19	794.898	12.5802
21	794.898	12.5802	20	794.898	12.5802
22	794.898	12.5802	21	794.898	12.5802
23	794.898	12.5802	22	794.898	12.5802
24	794.898	12.5802	23	794.898	12.5802
25	794.898	12.5802	24	794.898	12.5802

V= 10 TO 9 P- AND R-BRANCH TRANSITIONS FOR PRASEODYMIUM OXIDE

BIBLIOGRAPHY

1. Silfvast, W. T., "Metal Vapor Lasers", Scientific American, Feb, 1973

2. Rice, W. W., et al, "Metal Atom Oxidation Lasers", Los Alamos Scientific Laboratory, March, 1974

3. Sax, I. R., Dangerous Properties of Industrial Materials, 3rd Edition, Reinhold, 1968

4. Murray, L. G., Metal Oxidation Laser, Master's Thesis, Naval Postgraduate School, Monterey, CA, June 1974

5. Karev, V. N., et al, Report Number FTD-MT-24-93-71, Foreign Technology Division of Air Force Systems Command, Wright-Patterson AFB, Thin Films of the Rare-Earth Metals, Unclassified, 1969

6. Dennison, D. H., Tschetter, M. J., and Gschneidner Jr., K. A., "The Solubility of Tratalum and Tungsten in Liquid Rare-Earth Metal", Journal of the Less-Common Metals, Vol II, p. 423-435, 1966

7. Herzberg, G., Molecular Spectra and Molecular Structure I. Spectra of Diatomic Molecules, Second Edition, Van Nostrand, 1950

8. Green, D_2 W_+, "Vibrational Constants of the C^2 II, A^{12} , and X^2 Electronic States of LaO", Journal of Molecular Spectroscopy, Vol 40, p. 501-510, 1971

9. Ames, L. L., Walsh, P. N., White, David, "Dissociation Energies of the Gaseous Oxides of the Rare Earths", The Journal of Physical Chemistry, Vol 71, Number 8, p. 2707-2718, July 1967

10. Battelle Memorial Institute, The Properties of the Rare Earth Metals and Compounds, 1 May 1959

11. Chace, W. G., and Moore, H. K., Exploding Wires, Vols 1-4, Plenum Press, 1964

12. Chupka, W. A., Inghram, M. G., and Porter, R. F., "Dissociation Energy of Gaseous LaO", The Journal of Chemistry Physics, Vol 24, Number 4, p. 792-796, April 1956

13. Coleman, W. J. (Battelle Memorial Institute), Downward Vacuum Vapor Deposition of Rare Earths Onto Hollow Microspheres, (NVWL-1288), February 1970

14. Curzon, A. E., and Chlebek, H. G., "The Observation of Face Centered Cubic Gd, Tb, Dy, Ho, Er, and Tm, in the Form of Thin Films and Their Oxidation", Journal of Physics F: Metal Physics, Vol 3, p. 1-5, January 1973

15. Izrael'son, Z. I., Toxicology of the Rare Metals, Israel Program for Scientific Translations, LTD., 1967

16. Powell, C. F., Oxley, J. H., Blocher Jr., J. M., Vapor Deposition, Second Edition, Wiley & Sons, March 1967

17. Rare-Earth Information Center Letter DTD November 14, 1975 to Richard C. Feierabend, Subject: Advising of Enclosed Requested Rare Earth Metal Information, November 14, 1975

18. Samsonov, G. V., et al, "Production of Thin Films by Evaporation of Rare Earth Metals and Study of their Physiochemical Properties", Chemical Abstracts, Vol 76, p. 250, Number 28765W, 1972

19. Thin Films, 1963 Seminar, American Society of Metals, 1963

20. White, D., et al, "Thermodynamics of Vaporization of the Rare-Earth Oxides at Elevated Temperatures; Dissociation Energies of the Gaseous Monoxides", Symposium on Thermodynamic Nuclear Material, Vienna, 1962, Vienna International Atomic Energy Agency, 1962

INITIAL DISTRIBUTION LIST

		No. Copies
1.	Defense Documentation Center Cameron Station Alexandria, Virginia 22314	2
2.	Library Code 0212 Naval Postgraduate School Monterey, California 93940	2
3.	Department Chairman, Code 67 Department of Aeronautics Naval Postgraduate School Monterey, California 93940	1
4.	Prof. D. J. Collins, Code 67Co Department of Aeronautics Naval Postgraduate School Monterey, California 93940	1
5.	LT Richard C. Feierabend, USN 3321 Treelawn Drive Richfield, Ohio 44286	1

Thesis
F2524 Feierabend
c.1 Metal atom oxidation
laser.